Chapter 3

Predictive modelling of prospectivity for Pb-Zn deposits in the Lawn Hill Region, Queensland, Australia

Acknowledgement of Contributions

N.H.S. Oliver – normal supervisory contributions

Abstract

Different approaches can be combined to explore for mineral deposits, involving a combination of geodynamic modelling, mineral potential mapping, and mineral deposit studies, aiming to provide a comprehensive understanding of ore systems at all scales. This chapter is focused on the mineral potential aspect, exploring the interrelationship between a knowledge-driven approach, which uses subjective evidence based on expert knowledge, and a data-driven model based on Bayesian probabilistic reasoning. The limitations and strengths of these approaches provide an example of how blending human interpretation with computational models can be an effective way to aid exploration and ore genesis interpretation. The study is focused on the Lawn Hill Platform, Mount Isa Inlier, situated in Northwestern Queensland, Australia. The models are used to predict the mineral potential in the area, focussing on SEDEX (Sedimentary Exhalative Deposits) and VS (Vein style) Pb-Zn mineralisation. The results of the comparison of Knowledge-Driven (KD) models versus Data-Driven models (DD) indicate that the Century zinc deposit (the largest Pb-Zn mineral resource found in this region) occurs in the area with highest mineral potential for SEDEX-type ore. The Lawn Hill Region shows good mineral potential close to the Termite Range Fault, within areas marginal to known prospects and vein/lode hosted deposits. However, there are lower favourability sites suggesting significant potential in the Kamarga Dome. Integration of the KD- and DD-models is considered a potential way to more reliably assess the favourability of locating a Century-type system. Use of this combined technique suggests that the highest favourability of locating a shale hosted mineralisation similar to Century is close to this

deposit along the Termite Range Fault zone. One particularly prospective site has been identified north of the Edith cluster.

Keywords: Weights of Evidence, Mineral potential mapping, Mount Isa Inlier, Bayesian Probability, Century zinc deposit.

3.1. Introduction

Before the construction of a predictive model, which can be defined as representing the favourability or probability for occurrence of a mineral deposit of the type/style sought, a schematic subdivision has to be drawn depending on the type of inference mechanism considered. The two model types are: (1) knowledge-driven; and (2) data-driven. Knowledge-driven models may show expert dependency, because the judgment of an expert is required during the weighting of evidential information, which depends directly on the expert-knowledge derived from wide and inhomogeneous experience. In contrast, data-driven models are more objective tools that should be considered independent from expert judgment (Carranza and Hale, 2003); however partial subjectivity is introduced when establishing the initial conditions in the data driven case (Agterberg, 1974). Particular care has to be taken then when choosing these subjective variables, to guarantee objectivity in the DD-model. In this study, a combination of these two approaches is presented (KD and DD), in which subjective and objective models are combined to help the predictive exploration process of a Pb-Zn mineral system. The knowledge-driven model is based upon geological information that defines structural and lithological boundaries. Common knowledge related to Pb-Zn deposits is also considered during score assignment, to define favourability models for both VS and SEDEX-style mineralisation. This model is then compared with a data-driven model to further the understanding of how objective methods such as WofE (Weights of Evidence Modelling) effectively work within a Pb-Zn mineral district.

Knowledge-driven (KD) and data-driven (DD) modelling can be performed using different mathematical, computational approaches (e.g. Neural Networks, Genetic Algorithms, and Expert Systems). These are independent fields of computer science, born after the sharp decline of artificial intelligence (AI) investments, which occurred in the early 90s following the lack of significant progress in this field. Since then, a number of researchers contributed to the development of new applications based on such emerging areas, including data-driven models applied to mineral exploration (Singer and Kouda, 1996; Harris and Pan, 1999). These workers implemented neural-net algorithms to explore for Kuroko type deposits in the Hokuroku District, Japan. The application of Expert Systems based on probabilistic reasoning was also extensive. PROSPECTOR (Duda et al., 1978) is a good example of an expert agent capable of answering questions relative to the genesis of oil/mineral systems as a human would do. To clarify, an Expert System is a computer program that acts like an expert in a particular field of knowledge, usually a profession, such as geology or medicine. These novel methodologies became objects of criticism in the 90s. For instance, Wolf (1994) states that the rate of discovery in mineral exploration was not really benefiting from implementation of Expert Systems although a clear measure of their success rate was not possible at that time. If these systems were not successful as expected in practical applications, they did stimulate debate, especially between AI researchers and statisticians. Criticism of the formalism required to treat uncertainty contributed to a series of philosophical outcomes, which prepared the ground for the development of present probabilistic inference approaches such as the example proposed here. Recently, more successful applications have been presented in the literature (Raines, 1999; Brown et al., 2000; Asadi and Hale, 2001; Carranza, 2004; Agterberg and Bonham-Carter, 2005; Carranza et al., 2005).

To handle uncertainty the subjectivist or personalist Bayesian method was implemented (see Spiegelhalter, 1986). This method holds that probability statements may be made regarding any potentially verifiable proposition; whether a chance mechanism can be imagined or not. The only constraints are that probability statements should be coherent (Spiegelhalter, 1986). This approach appeared to be particularly suitable for expert systems as the representation of an inference mechanism was based on potentially verifiable propositions "hypotheses" that all had the same logical type (Spiegelhalter, 1986). The Bayes' rule is widely applied when dealing with different sources of uncertainty. These can be defined in terms of conditional probabilities, which are progressively updated as soon as new propositions with their own probabilities are added to the model.

Other probabilistic methods have been developed to address the problem of uncertainty and incompleteness of a database. For instance, a detailed discussion of the Dempster-Shafer belief functions (Shafer, 1976) is briefly revised in Spiegelhalter (1986) and more extensively discussed in Smets (1990) and Carranza and Hale (2003). The latter propose a stochastic model based on a combination of belief functions with the Weights of Evidence method firstly applied to mineral exploration by Agterberg (1989) (and also

Bonham-Carter et al., 1989; Bonham-Carter, 1994). This "hybrid" probabilistic model represents an alternative to exclusively knowledge- or data- driven models. Spiegelhalter (1986) argues in agreement with Smets (1990), that Dempsterian models are more appropriate when dealing with missing information. Smets (1990) proposes also a subdivision of probabilistic models based on the quality of the probabilistic measure available. With well known values the Bayesian model is considered to be the best representation of knowledge, whereas for more uncertain cases ULP (upper and lower probability) models, for example the Dempster's model, are proposed as an alternative.

In the data-driven model presented below, a Bayesian approach was used because of the good representation of knowledge (large number of mineral deposits/prospects, D = 82) and it was easier to implement propositional logic into an OO (Object Oriented) application developed using Microsoft Visual Basic Express (VBE) referring to the original FORTRAN programs presented in Bonham-Carter (1994). VBE is demonstrated to be a flexible environment, useful during sensitivity testing carried out to reduce and understand the control of known variables on uncertainty.

3.2. Geologic setting

The examined area is located south of the Gulf of Carpentaria in Northwestern Queensland, and covers approximately 4764.29 km^2 corresponding to the Lawn Hill Region 1:100.000 geological map published in 1982 by the Bureau of Mineral Resources (Fig. 3.1a). Exposed stratigraphic sequences are part of the Mount Isa Inlier, which is subdivided into three north-south trending structural belts (Carter et al., 1961; Blake, 1987): (1) Western Fold Belt, (2) Leichhardt-Kalkadoon Belt, (3) Eastern Fold Belt (Fig.

3.1b). These have distinctive geophysical signatures (Wellman, 1992) and are separated by regionally extensive transcurrent fault zones (Blake and Stewart, 1992). The Lawn Hill Region is part of the Lawn Hill Platform, which is included in the Western Fold Belt (e.g. Blake, 1987). The Mount Isa Inlier is well known for its mineral endowment, which hosts some of the largest Pb-Zn stratiform deposits in the world (e.g. Mount Isa, HYC, Century), and also several IOCG (Iron Oxide Copper Gold) deposits (e.g. Ernest Henry, Eloise, Starra). Common characters to this mineral endowment are the proximity of deposits and prospects to faults that were active during basin evolution (Neudert and McGeough, 1996; Betts and Lister, 2002), suggestive of a strong tectonic control of mineralising events (Betts et al., 2004), both synsedimentary and syntectonic.

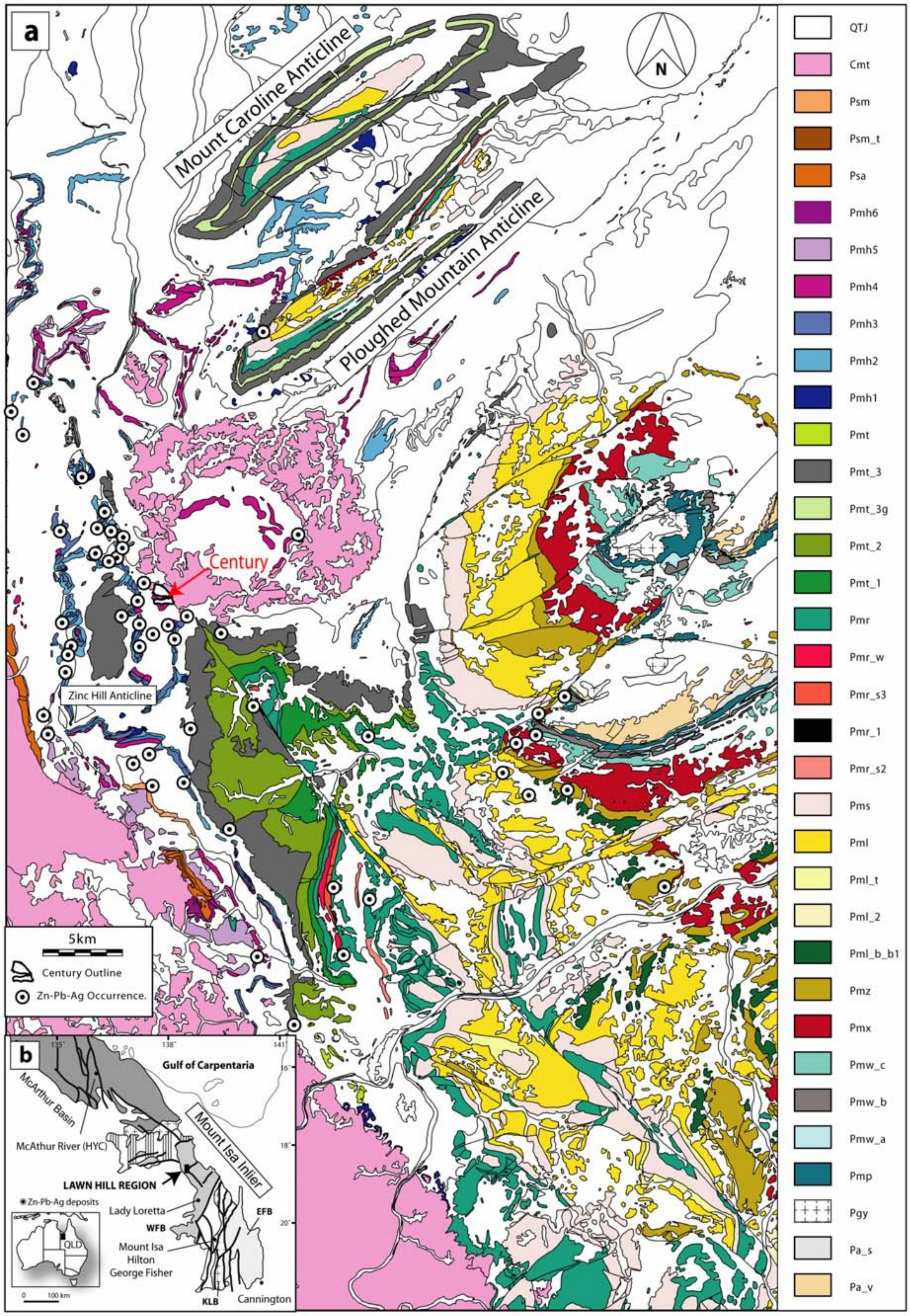
a
Mount Caroline Anticline
Ploughed Mountain Anticline
N
Century
Zinc Hill Anticline
5km
Century Outline
Zn-Pb-Ag Occurrence.
b
Gulf of Carpentaria
McArthur Basin
Mount Isa Inlier
McAthur River (HYC)
LAWN HILL REGION
Zn-Pb-Ag deposits
Lady Loretta
WFB
EFB
QLD
Mount Isa
Hilton
George Fisher
KLB
Cannington
100 km
QTJ
Cmt
Psm
Psm_t
Psa
Pmh6
Pmh5
Pmh4
Pmh3
Pmh2
Pmh1
Pmt
Pmt_3
Pmt_3g
Pmt_2
Pmt_1
Pmr
Pmr_w
Pmr_s3
Pmr_1
Pmr_s2
Pms
Pml
Pml_t
Pml_2
Pml_b_b1
Pmz
Pmx
Pmw_c
Pmw_b
Pmw_a
Pmp
Pgy
Pa_s
Pa_v

Fig. 3.1 Simplified geological map of the Lawn Hill Region (redrawn from the original 100:000 sheet). From youngest to oldest, (**QTJ**) Cainozoic and Mesozoic cover sediments. Quaternary (**Q**) sediments include alluvial clay, silt, sand, gravel. Tertiary (**T**) outcrops are mainly colluvium and residual soils, with variable degree of redbed oxidation. Alluvial sediments are also present with clay, silt and minor sand and travertine (Black clays). Sedimentary breccia and massive limestone close the basal part of the sequence. Jurassic rocks (**J**) are dominated by quartz-rich sandstones. Cherts, dolomites and phosphorites characterize the Cambrian period (**Cmt**). Mesoproterozoic South Nicholson Group lithotypes include siltstones and shales (Mullera Fm. – **Psm**) and hematitic, limonitic sandstones intercalated with shale beds (**Psm_t**). Conglomerate and sandstones represent the basal part of this group (**Psa**). Proterozoic Lawn Hill Fm. includes: (**Pmh6**) shale and flaggy siltstone-sandstone, (**Pmh5**) flaggy to blocky, micaceous and feldspatic sandstones; locally purple siltstones interbeds, (**Pmh4**) grey, fissile to flaggy siltstone and shale; flaggy tuff beds and minor dolomite, (**Pmh3**) flaggy to blocky, micaceous, lithic sandstones and conglomeratic sandstone, (**Pmh2**) fissile to flaggy tuff and tuffaceous siltstone, thinly interbedded siltstone, sandstone and shale, and (**Pmh1**) carbonaceous shale, flaggy siltstone interbeds and grey silty concretions; minor tuff. Termite Range Fm. includes: (**Pmt**) interbedded sandstone, quartzwacke, siltstone and shale, (**Pmt_3**) thick bedded, fine to coarse, poorly sorted sandstone and lithic greywacke interbedded with laminated siltstone, (**Pmt_3g**) medium to thick bedded, silicified quartzwacke interbedded with laminated siltstone and shale, (**Pmt_2**) thin to medium bedded, clayey siltstone and ferruginous sandstone, and (**Pmt_1**) thick-bedded, poorly-sorted sandstone and quartzwacke interbedded with siltstones. Riversleigh Siltstones Fm. includes: (**Pmr**) laminated and thin bedded, quartz-rich siltstones and shales, (**Pmr_w**) clayey siltstone and shale, (**Pmr_s3**) thin- to thick-bedded, quartz sandstone with clayey matrix; strongly cross-bedded, (**Pmr_l**) laminated quartz siltstone. (**Pmr_s2**) thick-bedded and silicified, dolomitic sandstones interbedded with siltstones. Shady Bore Quartzite (**Pms**) comprises orthoquartzites and sandstone with siltstone and dolomite interbeds. Lady Loretta Fm. includes: (**Pml**) thinly bedded to laminated intraclastic and stromatolitic dolomite with interbedded dolomitic siltstones and sandstones, (**Pml_t**) orthoquartzite, and (**Pml_b_b1**) breccia of chert and altered siltstones cemented by limonite; deeply weathered rocks. Esperanza Fm, (**Pmz**) consists of stromatolitic chert, siltstones, sandstones and dolomite. Paradise Creek Fm, (**Pmx**) is dominated by laminated and stromatolitic dolomites, dolomitic siltstone and sandstones; minor chert. The Gunpowder Creek Fm. includes: (**Pmw_c**) dolomite, dolomitic siltstone, oolitic dolomite, dolomitic sandstone, carbonaceous siltstone and sandstone, (**Pmw_b**) ferruginous arkosic sandstone, minor conglomerate, siltstone, stromatolitic dolomite, and (**Pmw_a**) micaceous siltstone, pyritic carbonaceous shale, siltstone and sandstone. Torpedo Creek Quartzite (**Pmp**) are predominantly massive sandstones, that becomes conglomeratic in the basal part. Yeldham Granite (**Pgy**) muscovite-rich leucogranite. Kamarga Volcanics includes: (**Pa_s**) feldspathic, conglomeratic and ferruginous sandstones, and (**Pa_v**) vesicular, amygdaloidal and massive basalt interbedded with feldspathic sandstones and conglomerates.

3.2.1. Tectonic evolution

Different tectonic models have been proposed to explain the geodynamic evolution of the Northern Australian Craton. Earlier models did not consider the structural implications of the intracratonic rifting history (Bell, 1983; Blake, 1987), explaining most of its structural features as a result of a major orogenic cycle (Mount Isa Orogeny, ca 1585-1500). Other workers developed geodynamic models based on detailed studies of fault architecture and basin history (e.g. Derrick, 1982; O'Dea et al., 1996; Betts et al., 1998; Scott et al., 1998b; Betts, 1999) providing new insights on the extensional characters of this terrain. The extensional evolution of the Mount Isa Inlier is best observed in the Western Fold Belt where the stratigraphic sequences are better preserved as regional shortening is less intense compared to the Eastern Fold Belt (Betts and Lister, 2002). Three extensional events were defined in chronological order: the Leichhardt Rift Event, the Myally Rift Event and the Mount Isa Rift Event (O'Dea et al., 1997; Lister et al., 1999; Betts, 2001). The Proterozoic extensional history was apparently terminated with the onset of the Isan Orogeny (ca. 1585-1500).

In the Western Fold Belt, the pre-existing basin architecture exerted strong control on the orientation of Isan Orogeny-related structures (O'Dea and Lister, 1995; Lister et al., 1999). Evidence of regional scale extension was derived from reconstructed stratal geometries of fault blocks; these are strongly asymmetric in cross-section exhibiting a pronounced rotational thickening and tilting, inferred to be related to listric faults. Interpreted unconformities cut down-section suggesting that differential uplift and rotation were responsible for their development (O'Dea et al., 1997). Other evidence of extensional tectonism was interpreted from the occurrence of doleritic intrusions along some listric faults, and syn-kinematic granitic intrusions that contributed to thermal anomalies that produced low-pressure, high-temperature metamorphism and extensive metasomatism in the region (Blake, 1987; Rubenach, 1992). The resulting geodynamic model invoked two cycles of intracontinental rifting each followed by metamorphism and crustal shortening (Barramundi and Mount Isa Orogeny) (O'Dea et al., 1997; Betts and Lister, 2001).

Scott et al. (1998b; 2000) and Southgate et al. (2000) proposed an alternative tectonic model based on sequence stratigraphic reconstructions and detailed geochronological constraints (e.g. Page et al., 2000). Rather than a rift-sag model they argue that extensional features, observed in the Mount Isa Inlier, could be explained as a local response to shear stress variation across major strike-slip faults active in a convergent setting. Development of strike-slip sub-basins was interpreted from isopach distributions and sequence stratigraphic thickness correlations (e.g. Krassay et al., 2000). Sub-basins were interpreted as potentially derived from increased accommodation during strike-slip deformation. However, Betts and Lister (2001) argued that the scale and influence of such tectonic activity was secondary, and cannot explain the broad distribution of half-graben structures within the Isa Superbasin. The large spatial and temporal distribution of half-grabens might be compared to the spatial and temporal extent of the Basin and Range province (Betts and Lister, 2001, 2002). This consideration coupled, for example, with the complex distribution of mineral deposits across the Mount Isa Inlier (Betts et al., 2003) led these workers to reinterpret these features as a result of prolonged activity within a back-arc dominated setting rather than a pure intracontinental rifting scenario. Intraplate, extensional deformation at regional scale may have been linked to the emplacement of a mantle plume (Oliver et al., 1991; Khain, 1992; Betts and Lister, 2001), promoting lithospheric thinning (Intracontinental rifting case) and steeper geothermal gradients. However, the evidence of a convergent margin preserved in the eroded remanents of the Strangways, Argilke and Chewings orogens (Collins and Shaw, 1995), and related arc magmatism (Zhao and McCulloch, 1995) led Betts et al. (2003) and Giles et al. (2004) to propose that basin development in Mount Isa was a consequence of far-field continental back-arc, extension. Subsequent basin inversion and tectonic reactivation occurred during local extensional relaxation of the lithosphere (Giles et al., 2004; Betts and Giles, 2006).

The controversy existing among these briefly introduced tectonic models is due to the often difficult interpretation of complex deformational features resulting from overprinting of extensional and compressional phases (e.g. Ploughed Mountain and Mount Caroline Anticlines, see Betts and Lister, 2002). Certain features (e.g. half-graben development) may also be diagnostic of either an extensional or compressional setting. In any case, within the Lawn Hill Platform the multiple styles of Pb-Zn mineralisation, likely reflect the interaction among the protracted reactivation history and concomitant hydrothermal events. The strong correlation of mineralisation with faulting hardly represents a pinpoint for the age of mineralisation in the Lawn Hill Platform, as faulting occurred throughout the entire structural evolution.

3.2.2. Style of faulting in the Lawn Hill Region

The Termite Range Fault (Fig. 3.1a, 3.2a) is the prominent structure in the study area, striking northwest for at least 70km in length (Hutton and Sweet, 1982). It was interpreted as one of the major conduits for mineralising brines that led to the formation of the Century zinc deposit, which is the major mineral resource in the Lawn Hill Platform, and (Andrews, 1998; Broadbent et al., 1998; Ord et al., 2002). The last significant offset, recorded along this fault, is relatively small (a few hundred meters) and displays a sinistral component of shearing (King, 2002). Some of the brittle deformation is interpreted as acting after the north-south folding (local D2, see Broadbent, 1999) as these shallow plunging folds (e.g. Zinc Hill Anticline, see Fig. 3.1a) are offset by northeast trending faults (e.g. Bresser, 1992; Broadbent, 1999). Northeast faulting is interpreted as synchronous with repeated activity (reactivation) of the Termite Range Fault, as these structures do not crosscut, neither offset this major discontinuity. Northeast faults are steep dipping with a dextral, transpressional strike-slip component (Bresser, 1992). Often they are prone to dilational step-over (see Sibson and Scott, 1998) and host significant concentrations of vein-style Pb-Zn ± Ag-Cu mineralisation (e.g. Silver King, Watson’s Lode, see Fig. 3.1a.). Most of these faults are sub-vertical suggesting that they may have, originally, formed as dip-slip structures developed during earlier stages of basin formation, within an extensional regime, and were contemporaneously active with the Termite Range Fault (e.g. Sibson, 1985a; Betts and Lister, 2002). This would explain their incompatible orientation if considered as Riedel shears of the Termite Range Fault (Hobbs et al., 1976).

E-W oriented faults are the third class of faults recognised in the region. Some of them (e.g. Pandora’s Fault – intersecting Century) display a normal component of slip. E-W discontinuities are poorly represented across the Lawn Hill Region and mostly are localised in well-defined structural domains (e.g. positive or negative flowers along the

Termite Range Fault). Therefore, at least some of them formed in response to local near-field stress conditions related to this fault. E-W faults appear sealed by m- to km-scale quartz veins, which are interpreted as forming either during or after strike-slip transpressional step-over (Fig. 3.2b). A number of lines of evidence suggest that all described fault systems were active in several periods during and after basin development: (1) fault dips are suggestive of formation in extensional conditions, whereas strike-slip off-sets are clearly post-folding (e.g. Zinc Hill Anticline); (2) the existence of km-scale folds (Ploughed Mountain and Mount Caroline Anticlines, Fig. 3.1a), with orientations incompatible with the broad stress tensors inferred to be approximately east-west (e.g. Broadbent et al., 1998; Betts and Lister, 2002), might be attributed to the reactivation of older basement faults (Betts and Lister, 2002) that formed during early rifting; (3) seismic profiles intersecting regional scale faults in the Northern Lawn Hill Platform (e.g. Elisabeth creek fault zone, Scott et al., 1998b) show that thickening of strata proximal to fault discontinuities developed during syn-depositional fault movement. The likely reactivation of faults represents a substantial issue either in term of definition of the timing of different fault generations and also when attempting to attribute a certain age to the mineralisation.

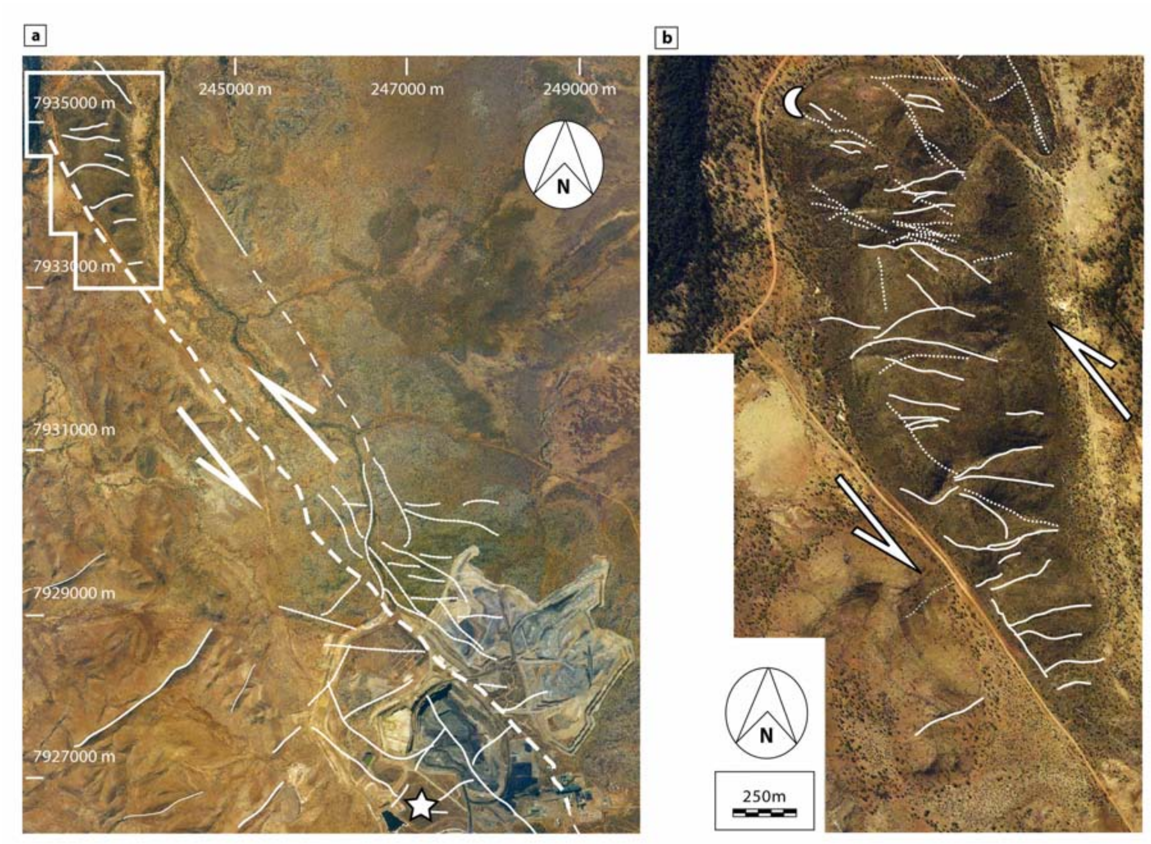

Fig. 3.2 Aerial photograph views illustrating the structural grain of the Century Area. (a) Prominent northwest and northeast striking faults in the study area. The Termite Range Fault (dashed lines) has anastomosed geometry indicative of its mature stage of reactivation. The fault displays sinistral shearing. Lateral splays of the fault apparently intersect the Century deposit (open cut). Local vein arrays are observed at the intersection of NW- and NE-faults south of Century (star symbol – see Fig. 3.6a and 3.6b). (b) Enlarged view of a contractional jog with interpreted faults. Outlined faults could be easily identified because of their quartz seals. A sinistral sense of shear is inferred considering the evidence of sinistral off-set in the Century pit area. A contractional scenario may also account for the presence of supra-lithostatic fluid pressures (jigsaw textures – moon site, see Fig. 3.6g).

3.2.3. Lawn Hill stratigraphy

Rocks exposed in the Lawn Hill Region comprise up to 8500 m of mildly deformed sediments that extend from the Murphy Tectonic Ridge in the north to the west of Mount Isa in the south (Hutton and Sweet, 1982). Bimodal suites of volcanic extrusives represent the basal part of these sedimentary packages and unconformably overlay older granitic intrusions, for example, the Yeldham Granite, outcropping in the southeastern corner of the Lawn Hill Region, approx. 1820 Ma, and the Big Toby granite, 1800 Ma (Wyborn et al., 1988; Scott et al., 1998b). O'Dea et al. (1997) discuss the subdivision in cover sequences previously mentioned and outlined in Fig. 3.3. Kamarga and Eastern Creek Volcanics overlying the basement granites are now regarded as part of the Haslingden Group (included in the Myally Supersequence interval, ca. 1780–1765 Ma). All these units are synchronous with the Leichhardt- and Myally-rift events (Betts et al., 1999). Cover sequences 3 and 4 unconformably overlie these sub-groups and can be subdivided into three distinct formations within the Lawn Hill Platform: (1) the Bigie Formation and Fiery Creek Volcanics and their equivalents; (2) the Surprise Creek Formation; (3) the McNamara Group. The Bigie Formation is characterised by predominantly coarse clastic hematitic units, mainly conglomerates and sandstones that were interpreted by Hutton and Sweet (1982) as product of shallow depositional, sabhka or playa lake settings that would account for the intense redbed oxidation of detrital iron. The Fiery Creek Volcanics are a rift-related suite of bimodal volcanics (Wyborn et al., 1988), which are intercalated with the Bigie Formation. Dating of the Fiery Creek Volcanics yields a U–Pb zircon eruption age of 1708 ± 2 Ma (Scott et al., 1998a). The Surprise Creek Formation comprises basal conglomerates and a sandstone facies that were deposited after uplift and erosion of the Fiery Creek Volcanics (Derrick et al., 1980; Hutton and Sweet, 1982; Betts et al., 1999). The Surprise Creek Formation fines upward, becoming more distal as testified by sandy intervals containing well-rounded pebbles (Hutton and Sweet, 1982). In the top part, this formation becomes silty and sandstone dominated. The McNamara Group which hosts the major mineral resources in the Lawn

Hill Platform (e.g. Century Pb-Zn-Ag deposit) can be subdivided in an upper and lower unit (Andrews et al., 1996). The lower unit has in its basal part a clastic component partly derived form reworking of underlain intervals (Torpedo Creek Quartzite). Following this alluvial phase a deeper marine setting is inferred from evidence of euxinic conditions dominated by intercalated siltstone and shales becoming particularly enriched in carbonaceous material in the Kamarga Dome Area (see Fig. 3.1a); these lithotypes represent the Gunpowder Creek Formation. This formation underwent uplifting, erosion and lateritisation (redbeds), followed by deposition of dolomites and cherts. Shallow water dominated settings persisted until deposition of the Shady Bore Quartzite and includes the following formations: (1) Mount Oxide Chert Member, (2) the Paradise Creek Formation, (3) the Esperanza Formation and (4) the Lady Loretta Formation. All these formations are particularly enriched in carbonates - predominantly dolomites, their textural appearance and grain-size represent the result of deposition in subtidal (below wave base) to supratidal conditions (Hutton and Sweet, 1982). Stromatolites and cross-laminated sandstones with ripple-marks, and rare pseudomorphs of evaporitic anhydrite are indicative of intertital to supratidal settings. Periods of fine grained low-energy subtidal deposition were defined by crystalline dolomites, cherts, siltstones and shales, which formed laminated beds. Local euxinic facies are observed; their restricted nature may be indicative of lagoonal settings and was apparently a favourable trap for mineral deposits, for example, the Lady Loretta Pb-Zn-Ag deposit (e.g. Large and McGoldrick, 1998). Its small tonnage and rich grades (8.3 Mt at 18.4% Zn, 8.5% Pb, and 125 g/t Ag) may be a direct function of such a depositional environment.

The upper part of the McNamara Group is marked by its more transgressive nature (Andrews et al., 1996), and can be subdivided in four main formations: (1) the Shady Bore Quartzite, (2) the Riversleigh Siltstone (3) the Termite Range Formation (4) and the Lawn Hill formation, which hosts the Century deposit in its upper member (Andrews et al., 1996; Andrews, 1998; Krassay et al., 2000). The Shady Bore Quartzite has similar connotation to the Lady Loretta Formation with lithotypes typical of marginal to shallow water settings (e.g. quartzose sandstones and dolomitic siltstones). A phase of transgression is initiated with the deposition of the Riversleigh Siltstone that progressively leads to more mid- to outer-shelf settings dominated by finer lithotypes. The transgressive episode continued during deposition of the Termite Range Formation although it has a more distal connotation as shelfal depositional textures are lacking. Andrews (1998) interprets these members as high concentration turbidites, in which control of provenance of sediment supply and grain-size variation may have partly been influenced by synsedimentary growth faults. This latter consideration is supported by more recent regional tectonic interpretations for the northern part of the Lawn Hill Platform (see Scott et al., 1998b), which documents possible syn-depositional faulting. The Lawn Hill Formation represents the terminal formation of the McNamara Group, and was originally subdivided into six members by Hutton and Sweet (1982) (classification adopted for the mineral potential maps presented below – Fig. 3.3) and three other sub-units were defined by Andrews. The sedimentation of the Lawn Hill Formation occurred predominantly in outer-shelfal to deep-water settings (Andrews, 1998), and it is characterised by sandstone, siltstone, and carbonaceous shale deposition. This is confirmed by the widespread abundance of siltstone and shale dominated facies that extends for several km- across the platform; therefore, being more typical of deep marine facies as Andrews (1998) interprets. Typical also is the intercalation of laminated shales and siltstones with volcaniclastic tuffaceous layers. Felsic activity may have been synchronous with episodes of tectonic extension of the Mount Isa Basin, which may have partly controlled depositional cycles. The initiation of the Isan Orogeny (approx. -1585 Ma) may have controlled uplifting during the later phases of deposition (e.g. Krassay et al., 2000). Fig. 3.3 presents a summary of these lithostratigraphic sequences.

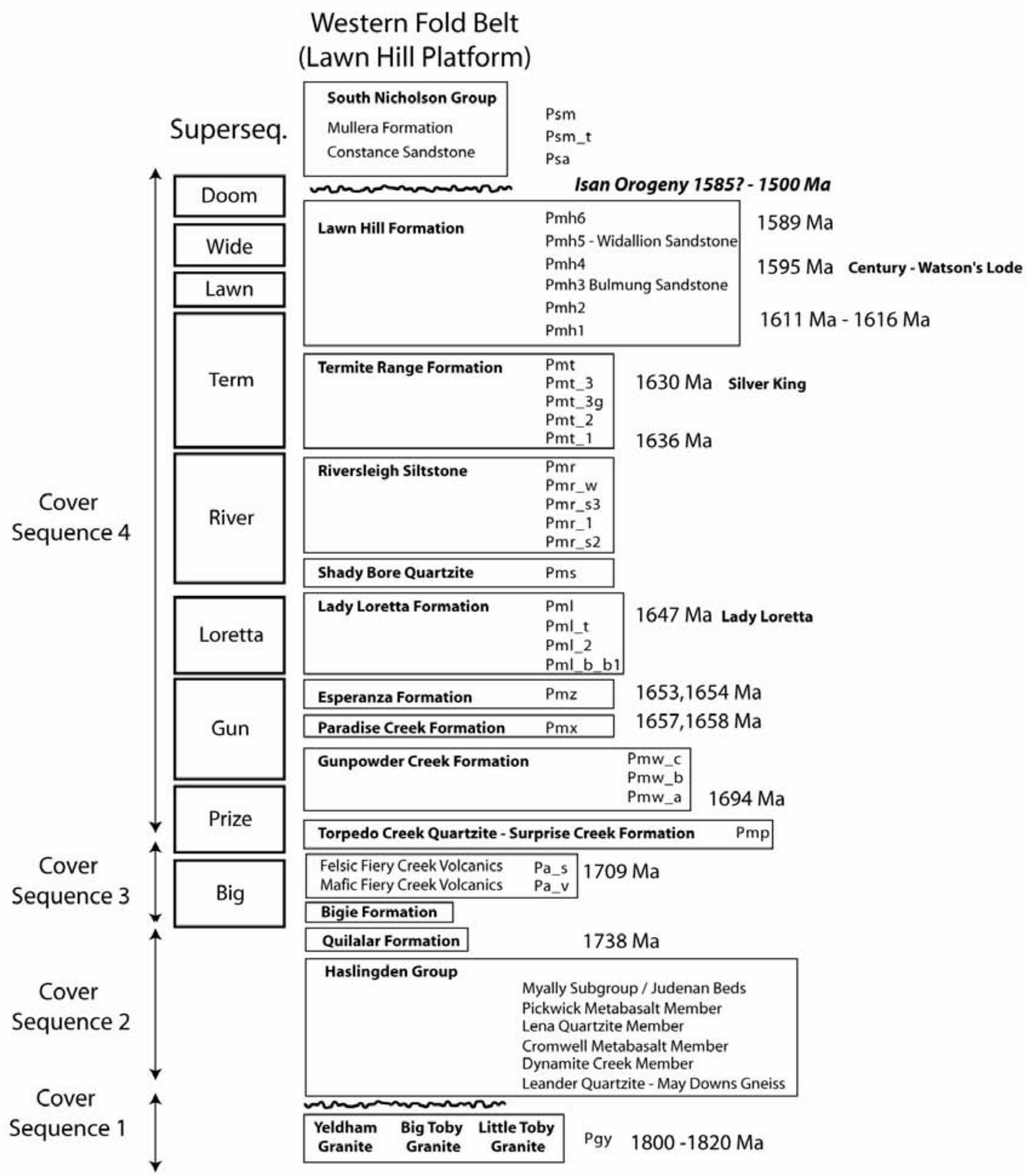

Fig. 3.3 Schematic diagram of the Lawn Hill Platform illustrating stratigraphic subdivisions of Hutton and Sweet (1982). This classification was adopted for both KD- and DD-models. For the DD- model, subunits were grouped accordingly with their formations (e.g. Pmh6 has been grouped as Pmh). The age of the Isan Orogeny is from Hand and Rubatto (2002). Sedimentary ages from Page et al. (2000). Supersequence classification from Krassay et al. (2000) and Southgate et al. (2000). Cover sequence subdivision from O'Dea et al. (1997).

Changes in the palaeogeographic conditions seem to exert a prominent control on the spatial distribution of Pb-Zn mineralisation in the Mount Isa Inlier. Pb-Zn massive sulphides appear spatially associated with organic rich lithotypes near supersequence boundaries. Therefore, even if Pb-Zn massive sulphides formed in different depositional settings or by different processes they share this commonality. Perhaps when comparing the spatial distribution of deep marine shales versus lagoonal type carbonaceous shales, the deeper settings may be more prospective because of their wider lateral extent. This could also account for the low tonnage occurrences found in restricted, shallower settings (e.g. Lady Loretta).

The deformational history (e.g. repeated activity of a fault system) needs also to be coupled with the sedimentary facies evolution to further constrain the search for Pb-Zn mineral deposits. In the next section a simple model is introduced that tries to answer the problem of integration of these parameters, in a 2D-GIS environment. The problem of investigating how tectonic and sedimentary components are uniquely associated with a certain style of mineralisation will also be discussed.

3.3. Mineral deposits characters and relative conceptual models

3.3.1. Deposit classification

This section provides a brief outline of the characters and ore genetic models typical of the different styles of Pb-Zn mineralisation observed in the Lawn Hill Region (Table. 3.1). Conceptual models are used to define the search criteria; this is followed by the favourability modelling. Detailed descriptions of mineral deposit characters are abundant in literature (e.g. Gustafson and Williams, 1981). Many workers concerned with Pb-Zn deposits have attempted to draw well defined boundaries between the various styles of Pb-Zn ore observed. However, it is common belief that many examples of Pb-Zn ores are transitional to the three classes of mineral deposits discussed here:

- **SEDEX model**
- **MVT model**
- **IRISH model**

There are however some substantial differences among these styles of mineralisation, these are:

- the depositional setting: for example we notice that MVTs and IRISH-style mineralisation are more typical of the carbonatic platform and shallow water shelfal settings, whereas SEDEX occurs more in deeper parts of a basin usually within restricted half-grabens as illustrated in Table 3.1.
- Additional differences are also the type of textural appearance of the mineralisation which is more coarse grained in MVTs and many IRISH deposits. However, the latter have also examples (e.g. Navan deposit) that effectively could be comparable to the very fine textural relationships and morphologies of sulphide species observed in laminated SEDEX deposits.
- Another important distinction is also the size and form of the three categories illustrated below. Apparently, SEDEX are the most laterally extensive as they

can be more than 1 Km in length. MVT have more irregular shape and occur often in less continuous fashion (100s of metres), because of the irregular network of fluid flow paths developed in limestone cavities and collapse breccias. IRISH-style ores appear to be a compromise between these two extremes; however, they are usually smaller in size than SEDEX being also apparently more focused within fault controlled settings.

Illustrated characters may be interpretable as the direct product of specific metallogenic patterns. In other words, as Kesler (1997) proposes, there are a number of parameters that control the final outcome of a metallogenic event. Deep crustal or mantle features may exert the strongest control on the type of mineral deposits. However, the actual style of deposits is controlled by upper crustal features, particularly the relative abundance of carbonate and silicate in the country rock. Therefore, different typologies of deposits might be considered a direct example of upper crustal controls.

In addition to tectonic and petrologic factors, Kesler (1997) remarks that global forcing mechanisms such as global anoxia and plate reorganisations should also be considered. Certainly the role of global anoxia has produced deep water environments that favoured the formation of SEDEX mineralisation either on the seafloor (or subsurface, if the anoxic water recharged underlying aquifers). These rare events in the geological record may be responsible for the uniqueness of certain deposits. For example, we might consider an intracontinental back-arc system – the Okinawa trough in the Japan Sea. This hydrothermally active region is the only modern day example of an evolving back-arc scenario involving continental crust (Glasby and Notsu, 2003). Such a tectonic scenario could be compared with the early stages of extension and sagging observed in the Mount Isa Inlier, although substantial differences may exist in term of tectonic organisation of the continental margin and also some of the features observed in the petrology and metal endowment in the Mount Isa Inlier may also be function of the later orogenic overprint. Nonetheless, the size of mineral deposits in the Jade field, Okinawa trough, appears to be smaller (the largest ore body in the Jade field is a few tens of metres in diameter and 15 m high and has a total area of 0.2 Km^2) compared to the Mesoproterozoic examples, such as Century, HYC or Mt. Isa (Century exceeds 3 Km^2). Global forcing mechanisms may then have been a requirement to obtain such giant ore bodies, as modern examples seem to be lacking.

Table 3.1. Summary of the broad characteristics of SEDEX, IRISH-style and MVT deposits.

	SEDEX - Sedimentary Exhalative Zn-Pb-Ag	*IRISH - Type, Carbonate hosted Zn-Pb*	*MVT - Mississippi Valley Type, Carbonate hosted Zn-Pb*
General description	*These deposits are stratiform in nature with beds and laminations of sphalerite, galena, pyrite, pyrrhotite and rare chalcopyrite, with or without barite, in euxinic clastic marine sedimentary strata. Deposits are typically tabular to lensoidal in shape and range from centimetres to tens of metres thick. They can also occur in multiple lenses at considerable distance from one another*	*Irish-type carbonate-hosted deposits are stratabound, massive sphalerite, galena, iron sulphide and barite lenses with associated calcite, dolomite and quartz gangue in dolomitised platformal limestones. Deposits are structurally controlled, commonly wedge shaped adjacent to normal faults. Deformed deposits are irregular in outline and commonly elongate parallel to the regional structural grain.*	*Mineral deposits are stratabound and have relatively simple mineralogy, with galena and sphalerite as the main ore minerals nearly always accompanied by pyrite and/or marcasite. Barite and fluorite are common in some districts. Chalcopyrite is a minor associate. Deposits commonly develop within breccias or palaeokarst topography in platformal carbonates. They are also found at the interface between carbonates and shales.*
Tectonic setting	*Intracratonic, or continental margin in fault controlled throughs. Troughs are typically half grabens developed by extension along continental margins or within back-arc basins*	*Platformal sequences on continental margins which commonly overlie deformed and metamorphosed continental crustal rocks.*	*Deposits tend to be found at or near the edges of basins as presently preserved or on arches between basins.*
Depositional environment	*The depositional environment varies from deep, starved marine to shallow water shelfal setting. There is often evidence of penecontemporaneous movement of faults bounding sites of sulphide deposition.*	*Adjacent to normal growth faults in transgressive, shallow marine platformal carbonates near basin margins.*	*They may occur in relatively undisturbed platformal carbonates or within foreland fold and thrust belts.*
Age of mineralization and host	*The major metallogenic events are Middle Proterozoic, Early Cambrian, Early Silurian and Middle to Late Devonian to Mississippian. The Middle Proterozoic and Devonian-Mississippian events are recognised worldwide.*	*Known deposits are believed to be of Palaeozoic age and younger their host rocks; Irish deposits are hosted by Lower Carboniferous rocks; Kootenay Arc deposits are in the Lower Cambrian.*	*Host rocks range in age from Proterozoic to Cretaceous, although many fewer deposits are known in the Proterozoic, Jurassic and Cretaceous than in the Cambro-Ordovician and Carboniferous.*

	SEDEX - Sedimentary Exhalative Zn-Pb-Ag	IRISH - Type, Carbonate hosted Zn-Pb	MVT - Mississippi Valley Type, Carbonate hosted Zn-Pb
Host/Associated rock types	*The most common host-rocks are those found in euxinic, starved basins, namely carbonaceous black shale, siltstone, cherty argillite and chert. Thin interbeds of turbiditic sandstone, granule to pebble conglomerate, pelagic limestone and dolostone, although volumetrically minor are common. Evaporites, calcareous siltstone and mudstone are common in shelf settings. Slump breccia, fan conglomerates and similar deposits occur near synsedimentary growth faults. In some basins high-level mafic sills with minor dikes are important.*	*Hosted by thick, non-argillaceous carbonate rocks; these are commonly the lowest pure carbonates in the stratigraphic succession. They comprise micritic and oolitic beds, and fine-grained calcarenites in calcareous shale, sandstone, calcarenite succession. Underlying rocks include sandstones or argillaceous calcarenites and shales. Iron formations, comprising interlayered hematite, chert and limestone, may occur as distal facies to some deposits. Deformed Kootenay Arc deposits are enveloped by fine grained grey, siliceous dolomite that is generally massive or only poorly banded and locally brecciated.*	*Although early workers commonly suggested that deposits were located within carbonate reef masses, subsequent work as shown that only a few of them are found in this setting. MVT are closely controlled by the prior development of porosity, and thus may be located in platformal carbonates of biostromal character, back-reef or fore-reef settings are also preferential sites of mineralisation.*
Deposit form	*These deposits are stratiform but also stratabound, with tabular to lens shaped morphology. Sulphides and/or barite occur often in laminae that extend for several metres to 100s of metres. Usually lateral extent is more than the vertical extent.*	*Deposits are typically wedge shaped, ranging from over 30 m thick adjacent to, or along growth faults, to 1-2 cm bands of massive sulphides at the periphery of lenses. Economic mineralisation rarely extends more than 200 m from the faults. Large deposits comprise individual or staked sulphide lenses that are roughly concordant with bedding. In detail, however, most lenses cut host stratigraphy at low angles. Contacts are sharp to gradational. Deformed deposits are typically elongated within and parallel to the hinges of tight folds.*	*Highly irregular. May be peneconcordant as planar, braided or linear replacement bodies. May be discordant in roughly cylindrical collapse breccias. Individual ore bodies range from a few tens to a few hundreds of metres in the two dimensions parallel with bedding. Perpendicular to bedding, dimensions are usually a few tens of metres. Deposits tend to be interconnected thereby blurring deposit boundaries.*

	SEDEX - Sedimentary Exhalative Zn-Pb-Ag	IRISH - Type, Carbonate hosted Zn-Pb	MVT - Mississippi Valley Type, Carbonate hosted Zn-Pb
Texture/Structure	Sulphide and barite laminae are usually very finely crystalline where deformation is minor. In intensely folded deposits, coarser grained, recrystallized zones are common. Sulphide laminae are typically monomineralic.	Sulphide lenses are massive to occasionally well layered. Typically massive sulphides adjacent to faults grade outward into veinlet-controlled or disseminated sulphides. Colloform sphalerite and pyrite textures occur locally. Breccias are common with sulphides forming the matrix to carbonate (or as clasts). Sphalerite-galena veins, locally brecciated, commonly cut massive sulphides. Rarely (Navan), thin laminated, graded and crossbedded sulphides, with framboidal pyrite, occur above more massive sulphide lenses. Strongly deformed sulphide lenses comprise interlaminated sulphides and carbonates which, in some cases, has been termed shear banding.	Most commonly as sulphide cement to chaotic collapse breccia. Sulphide minerals may be disseminated between breccia fragments, deposited as layers atop fragments ("snow-on-roof"), or completely filling the intra-fragment space. Sphalerite commonly displays banding, either as colloform cement or as detrital layers ("internal sediments") between host-rock fragments. Sulphide stalactites are abundant in some deposits. Both extremely fine-grained and extremely coarse-grained textured sulphides minerals may be found in the same deposit. Precipitation is usually in the order pyrite (marcasite) →sphalerite → galena.
Ore mineralogy	(Principal and subordinate): The principal sulphide minerals are pyrite, pyrrhotite, sphalerite and galena. Some deposits contain significant amounts of chalcopyrite, but most do not. Barite may or may not be a major component of the ore zone. Trace amounts of marcasite, arsenopyrite, bismuthinite, molybdenite, enargite, millerite, freibergite, cobaltite, cassiterite, valleriite and melnikovite have been reported from these deposits. These minerals are usually present in very minor amounts.	(Principal and subordinate): Sphalerite, galena; barite, chalcopyrite, pyrrhotite, tennantite, sulfosalts, tetrahedrite, chalcopyrite.	(Principal and subordinate): Galena, sphalerite, barite, fluorite. Some ores contain up to 30ppm Ag. Although some MVT districts display metal zoning, this is not a common feature. The Southeast Missouri district and small portions of the Upper Mississippi Valley district are unusual in containing significant amounts of Ni-, Co-, and Cu-sulphides.

3.3.2. Conceptual models

Several conceptual models have been proposed to explain the defined styles of Pb-Zn mineralisation. Beside the control exerted by the host rock, substantial debate among researchers concerns the source of metals, the type of fluids transferring metals, the structure of hydrothermal systems, and also the primary driving forces that caused fluids to move in the crust (in some districts for 100s of kilometres), and their relationship to the geothermal, salinity and hydraulic gradients. For instance, the role of mantle plumes, or upper crust melting with relative intrusive activity and volcanism have been proposed as possible causes of the large convection systems required to source and concentrate metals in the sites of deposition (Solomon and Groves, 1994). Also the role of topographic uplift in creating hydraulic gradients capable of transferring fluids for large distances was considered among the possible mechanism for driving fluids (e.g. Garven, 1985). Finally, for the Irish districts, it has been proposed and questioned that the fluids interacted with basement to extract Pb-Zn (Oliver et al., 2006). Classical models are then reviewed in following sections to explore some of these topics.

3.3.2.1. SEDEX and IRISH

Similar ore genetic models are commonly proposed for sediment hosted exhalative deposits and Irish-style ores:

(1) syngenetic seafloor deposition (e.g. Goodfellow et al., 1993): evidence for syngenesis includes stratiform geometry of some deposits, occurrence together of bedded

and clastic sulphides, sedimentary textures in sulphides, and, where determined, similar ages for mineralization and host rocks;

(2) diagenetic to epigenetic replacement: replacement and open-space filling textures, lack of laminated sulphides in most deposits, alteration and mineralization above sulphide lenses, and lack of seafloor oxidation.

In these models it is mainly the fluid mixing and interaction with the host rock that causes base metal fixation. Hydrothermal fluids may derive directly from seawater that, penetrating at depth, recharges aquifers and increases its temperature according to the geothermal gradient. The gradient can be anomalous if plumes or intrusive/extrusive activity is proximal or if large convection cells transfer laterally thermal energy away from magmatic sources. High salinities especially Cl^- facilitate the enrichment and transport of metals (Pb-Zn-Cu-Ag-Au etc.). Brines can travel for considerable distances until they encounter a major discontinuity that connects aquifers allowing fluids to ascend and encounter fresh sea-water and/or suitable host rocks that can interact with them causing ore deposition. In this context, essential parameters are an extensive network of aquifers, which are the primary source of metals, a major fault that act as a fluid flow driver focussing fluids, and finally a trap where by either mixing with other fluids and/or whole rock-reactions metals accumulate efficiently.

3.3.2.2. MVTs

Mississippi Valley Type deposits are epigenetic, having been emplaced after host rock lithification. Ore hosting breccias are considered to have resulted from dissolution of more soluble sedimentary units, followed by collapse of overlying beds. The major mineralizing processes appear to have been open-space filling between breccia fragments, and replacement of fragments or wall rock. The relative importance of these two processes varies widely among, and within, deposits. Fluid inclusion data show that these deposits formed from warm (75°- 200°C), saline, aqueous solutions similar in composition to oil-field brines. Brine movement out of sedimentary basins, through aquifers or faults, to the hosting structures is the most widely accepted mode of formation (e.g. Garven and Freeze 1984a, b; Garven, 1985).

Two main processes have been proposed to move ore solutions out of basin clastics and into carbonates:

A. compaction-driven fluid flow generated by over-pressuring of subsurface aquifers by rapid sedimentation, followed by rapid release of basinal fluids (see Jackson and Beales, 1967), and

B. gravity-driven fluid flow which flushes subsurface brines by artesian groundwater flow from recharge areas in elevated regions of a foreland basin, to discharge areas in regions of lower elevation (e.g. Garven, 1985).

In addition to fluid transport, three geochemical mechanisms have been proposed to account for chemical transport and deposition of ore constituents:

1. *Mixing* - Base metals are transported by fluids of low sulphur content. Precipitation is caused by mixing with fluids containing hydrogen sulphide, replacement of diagenetic iron sulphides, and/or reaction with sulphur released by thermal degradation of organic compounds.

2. *Sulphate reduction* - Base metals are transported together with sulphate in the same solution. Precipitation is the result of reduction of sulphate by reaction with organic matter or methane.

3. *Reduced sulphur* - Base metals are transported together with reduced sulphur. Precipitation is brought about by change in pH, dilution, and/or cooling.

In all models structure and reactive hosts are the main controlling parameters for the deposition of Pb-Zn ore bodies. These aspects formed the basis for the prospectivity modelling of the Lawn Hill Region. Individual deposit attributes listed in Tab. 3.1 are chosen and explained in their role in the prospectivity models (below).

3.4. Knowledge driven modelling

A knowledge-driven model can be considered a conceptual model that involves a component of generalisation, and uncertainty (Harbaugh and Bonham-Carter, 1970). Experienced geologists have to take in consideration these elements when drawing their conclusions. The conceptual model can be based entirely on human inferences and their testing, although also empirical testing can be carried out using computer-based simulation (e.g. numerical modelling, Ord and Oliver, 1997; Mair et al., 2000; Oliver et al., 2001; McLellan et al., 2004; Miller and Wilson, 2004).

A data structure (Bishop et al., 1975) was created to simplify the definition and organisation of parameters (n-variables) (Fig. 3.4). The source of information used for this KD-model can be subdivided into structural and lithological. The first includes field observations, structural information derived from available digital maps and 3D models, and knowledge of mineralisation and faulting in the region. Individual lithostratigraphic intervals were derived from the geological map of the Lawn Hill Region and from selection and re-compilation of data collected within the NABRE project (Northern Australian Basin Research Evaluation project, Southgate, 2000).

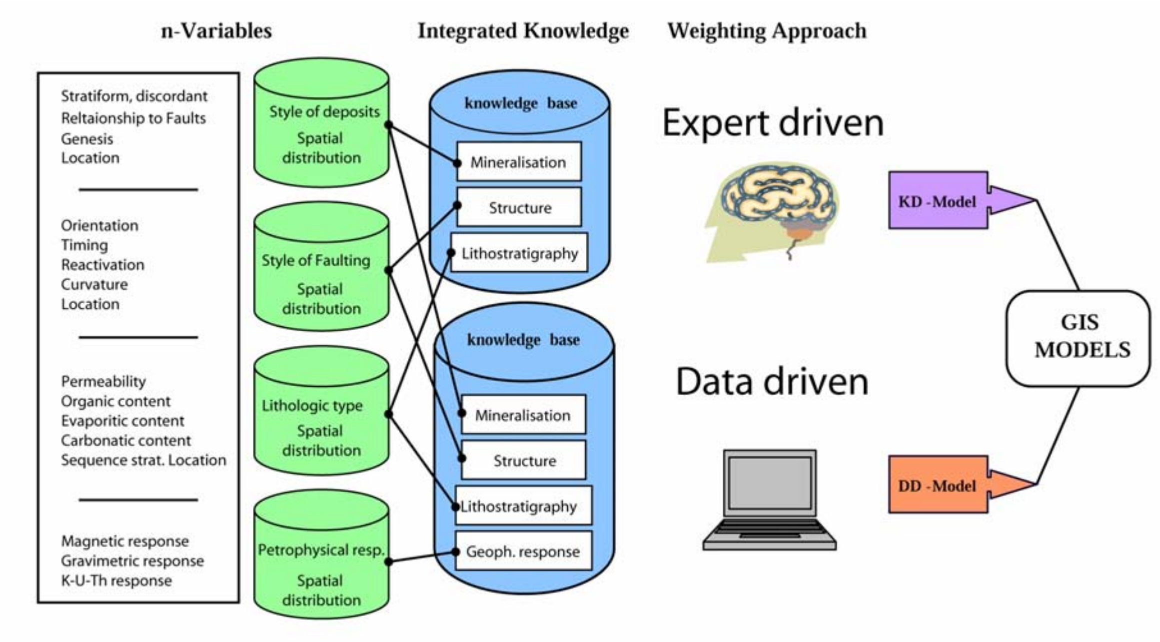

Fig. 3.4 Conceptual model used to generate a data structure to perform the KD- and DD-modelling of mineral potential. n-variables represent parameters inferred to be controlling features for the mineralisation. Each n-variable can be grouped in clusters of variables, which comprise a descriptive component and its spatial distribution. Components represent the knowledge-base that an expert or a computer program can use to develop inferences. These can be expressed as GIS models.

3.4.1. Deformational control on mineralisation

The structural component of the KD-model is examined here, focussing on the influence of faulting on mineralisation. To understand the role of faulting it is essential to firstly understand the style of mineralisation. The Lawn Hill Region hosts two main styles of mineral deposits containing extremely massive to sub-economic concentrations of Pb-Zn-Ag ore:

(1) Laminated/banded massive sulphides (stratiform nature), the most outstanding example being the world class, shale hosted Century zinc deposit (138 Mt at 8.23% Zn, 1.16% Pb, and 29 g/t Ag; Kelso, personal communication, 2003) (Fig. 3.1a).

(2) Structurally controlled veins/lodes, often occurring as agglomerated clusters of occurrences with small tonnage (e.g. Silver King-type), with predominantly Pb-Zn ± Ag-Cu. The latter are found in the surroundings of Century, but also, elsewhere (e.g. Flat Tyre prospect). Ore styles are also distinct by age and paragenesis (Richards, 1975; Bresser, 1992; Broadbent, 1999; Feltrin et al., 2004; Feltrin and Oliver, 2004).

3.4.1.1. Stratiform mineralisation

Many mineral deposits containing zinc, lead, copper, barium and/or precious metals are stratiform in that their general morphology is similar to sedimentary strata (Stanton, 1972; Morganti, 1981). The Century zinc deposit as for other several Pb-Zn deposits in the Mount Isa Inlier (e.g. HYC, McArthur Basin) is stratiform according to this definition. The spatial distribution of ore with respect to its host has been used frequently to attribute certain timing to the mineralisation although the acceptance of evolutionary concepts such as remobilisation, which causes secondary redistribution of sulphides, precludes the use of these geometrical arguments. A summary of Century's features is provided here; see Broadbent (1999) for detailed description of petrographic relationships. The Century Zn-Pb-Ag deposit occurs within an approximately 45 m thick interlayered black shale and siltstone in the Upper Lawn Hill Formation, within unit Pmh4 of Hutton and Sweet (1982). Andrews (1998) reclassified these in two sub-members (H4s, r) now considered part of the Wide Supersequence (Krassay et al., 2000).

Century has relatively simple sulphide mineralogy (Waltho et al 1993, Broadbent et al. 1998) with sphalerite, galena and pyrite as main mineralogical phases (Fig. 3.5a-d). Sulphides occur in multiple generations (Broadbent, 1999). This is also indicated by multiple generations of carbonates that overprint and form contemporaneously with sulphides of different timing (Broadbent et al., 1998; Feltrin and Oliver, 2004). Sphalerite has exceptionally pure stoichiometric compositions (Broadbent, 1999), and is frequently finely bedded (mm-scale) and mixed with different proportions of organic carbon (porous, non-porous sphalerite, see Broadbent et al. 1998). Galena occurs as fine grained, disseminated, euhedral crystals that forms bedded laminae. It occurs also in veins associated with sphalerite, galena, siderite and quartz. Deformational textures are also observed and can be interpreted as examples of remobilisation. Galena is the easiest sulphide to be mechanically displaced and plastically deformed by shearing (Fig. 3.5a, d). Pyrite occurs in very fine-grained size from millimetres to micrometres, displaying framboidal aggregates. These characters are typical of a seafloor or early-diagenetic setting, as formation of framboidal pyrite has been documented in the first few meters of the seafloor (e.g. Bertolin et al., 1995). However, the development of other generations of pyrite (late-diagenetic to syntectonic) is evident, as pyrite also occurs in veins (e.g. Fig 3.5b-c). The deposit comprises two stratiform lenses of massive, laminated to disseminated sulphides (H4r sub-unit), which are proximal to the Termite Range Fault, although their relationship with this major fault is less obvious compared to other giant ore deposits. For example, at the HYC deposit, interlayered mineralised talus breccias host graded sulphides (Large et al., 1998). At Century, evidence of synsedimentary breccias interbedded with mineralised black shale and siltstones could be inferred from reworked, tuffaceous layers hosting lobate to angular, autochthonous clasts of monomictic breccia. However, their origin is arguable as they could be due to syn- to post-depositional shearing along bedding planes (Fig. 3.5e).

Several sub-ordinate faults intersect Century. They have an orientation compatible with the Termite Range Fault, but also other regional-scale trends. They apparently postdate laminated mineralisation. Fault associated stringer zones are lacking at Century (e.g. Gecko Fault, Fig. 3.5f) although evidence of fracture controlled mineralised veins is documented in restricted portions of the mineral deposit (Fig. 3.5b, 5c and 5d). However, veins often appear unrelated to major faults at meso-scale. There is also lack of major reaction fronts which would be suggestive of a likely spatial association between stratiform mineralisation and faulting. Most of the mapped faults intersecting the mineral deposit appear to have formed well after its formation.

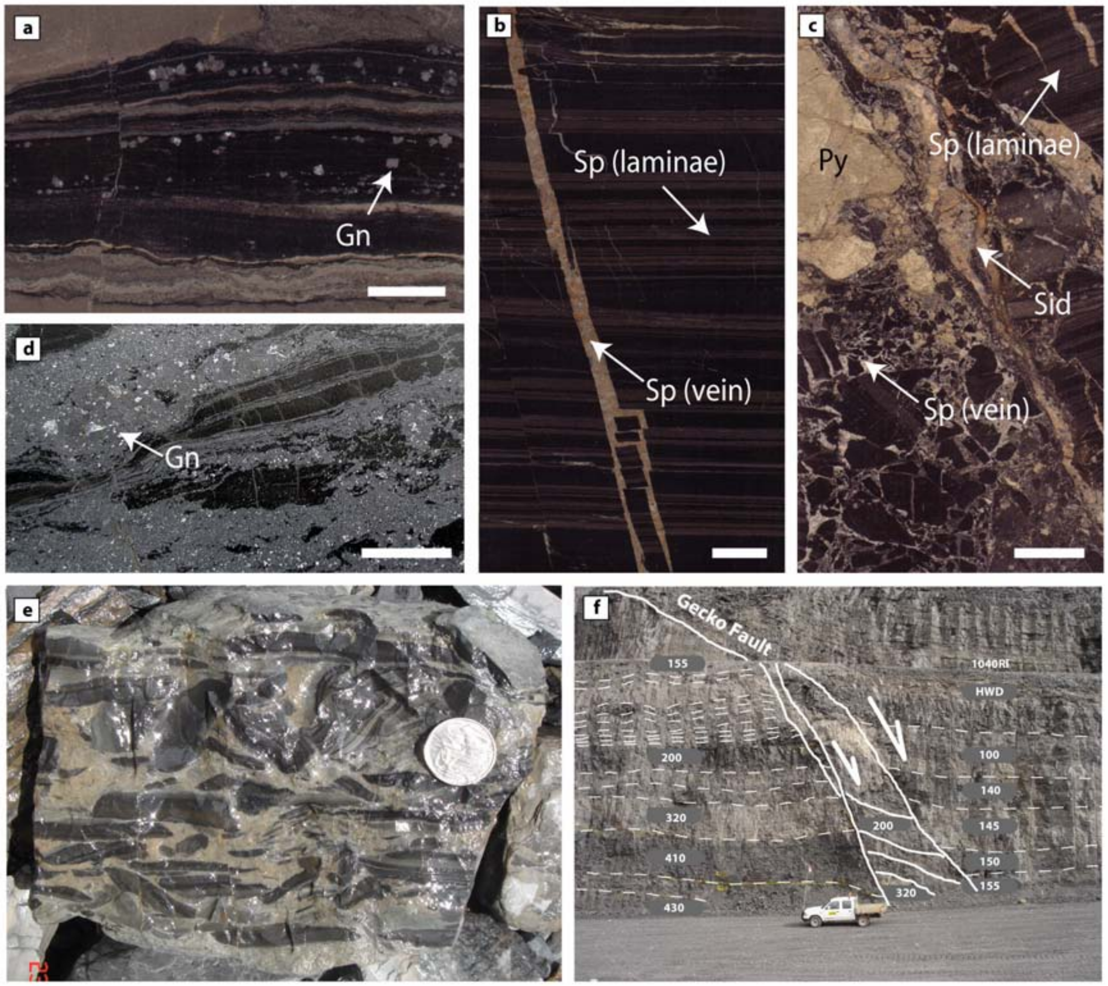

Fig. 3.5 Example of Century-style mineralisation and later deformational overprint. (a) Disseminated coarsen euhedral, cubic, galena (arrow, Gn). This was interpreted as the earliest phase of mineralisation at Century (e.g. Broadbent, 1999); however, at least part of the disseminated galena may have formed in a late syn- to post-diagenetic phase either postdating or being synchronous with discordant sphalerite (Sp- veins) (b), and also later pyritic (Py) phases (c). (d) Example of discordant galena (Gn) veins. (e) Example of siltstone/shale breccia with monomictic clasts floating in a tuffaceous sandstone, some clasts preserve earlier folding events, although glide folds may have formed relatively early during initial depositional phases. The specimen could be interpreted either as the product of synsedimentary brecciation or later tectonic related shearing originated from mechanical sliding localised in less cohesive tuff-intervals. (f) Open-pit exposure with highlighted mine stratigraphic intervals hosting the Century ore (e.g. unit 200). The deposit is intersected by later faults that apparently post-dates the mineralisation (scale bars in a, b, c, and d, 1 cm) (Appendix D for specimens spatial location).

3.4.1.2. Regional scale veins and lodes

Veins are one of the closest lines of evidence of the interplay between mineral species and fluids percolating a rock mass. They form in response to density imbalance, for example, induced by deformation. Vein-style mineralisation is widespread in the Lawn Hill Mineral Field, and has variable mineralogical composition (Fig. 3.6a-6g). This appears to reflect partly the variation of the host rock suggesting at least some local sources of infill (e.g. Bons, 2001; Oliver, 2001). For example, sandstone/siltstone-rich intervals (e.g. Termite Range Fm.) are frequently cross-cut by quartz-chlorite rich assemblages, whereas carbonaceous and carbonate-bearing shales appear to be more associated with quartz-rich, but also carbonate-rich infill (dolomitic to sideritic) (Fig. 3.6a, b). Siderite is found frequently associated with sulphides at Century, whereas quartz intermixed with sulphides are prominent in vein-hosted deposits. The paragenetic evolution of two major vein/lode Pb-Zn-Ag mineral occurrences (Silver King and Watson's Lode) is discussed in detail by Bresser (1992) who distinguish six paragenetic stages. The ore and alteration assemblage consists of quartz, carbonate (siderite, ankerite), sphalerite, galena, pyrite and minor chalcopyrite, either forming massive or fibrous vein intergrowths. Sulphides and gangue minerals form also colloform or comb (fine-grained layered) textures suggestive of mineral precipitation in open space, at shallow-depths of formation (Cox et al., 1987) (e.g. Fig. 3.6c, d, e). They also locally display crack-seal textures with infill of consistent mineralogy (Fig. 6f), suggesting a syn-deformational origin. In some cases vein fibres display also more complex patterns derived from syn-kinematic rotational components (King, 2002). Bresser (1992) reports 46 fluid inclusion analyses from main sphalerite phases at Silver King and also sphalerite and quartz at Watson's lode. These yield homogenisation temperatures within a range of 110 to 130°C. The salinity range is from 6.3 wt% to 21.3 wt%, equiv. NaCl, which is consistent with other MVT-type Pb-Zn deposits (e.g. Red Dog, Alaska). Leach et al. (2004) provide a comparison between deposits from Red Dog (Brooks Range, Alaska) and these regional lodes proximal to Century. Using bulk extraction ion chromatography, fluid inclusions of Silver King and Watson's lode are remarkably similar to the Red Dog deposit, with elevated Cl/Br ratio indicating derivation from evaporated seawater (Leach et al., 2004). Cl/Br molar values for the Silver King deposit inclusions are suggestive of original seawater dominated brines with elevated salinities between 30-35%. Fluid inclusions salinity range of 6.3 wt% may indicate therefore dilution, probably occurring through mixing with other fluids as inferred by Bresser (1992). The vein/lode systems were strongly controlled by faults that remained open for sufficient time to allow mineralisation in response to vertical channelised flow (Sibson and Scott, 1998). The depth of formation of this mineralisation is probably shallow considering the seawater dominated signature of the brines and the evidence of colloform textures indicative of open space conditions. Dilational step-over operated likely during later compressional tectonics, mostly favouring the opening of northeast fault arrays located west of the Termite Range Fault where vein style prospects and small deposits are clustered. However, evidence of hydrothermal activity is also documented close to the Termite Range Fault and seems to be associated with this major fault. Vein style mineralisation also intersects the Century deposit on its northeastern side (Waltho and Andrews, 1993; Feltrin et al., 2004; Feltrin and Oliver, 2004). The complex series of stages of deformation along faulted corridors involved brittle fracturing of pre-existing veins that resulted in complex patterning with formation of vein arrays (e.g. Fig. 3.6a and 3.6b). Sealed, dilational jogs (Sibson, 1985b) and jigsaw breccias (Fig. 3.6f, g) suggest that fluid pressures probably exceeded the tensile strength along fault margins, favouring hydrofracturing in response supra-lithostatic pore pressure gradients.

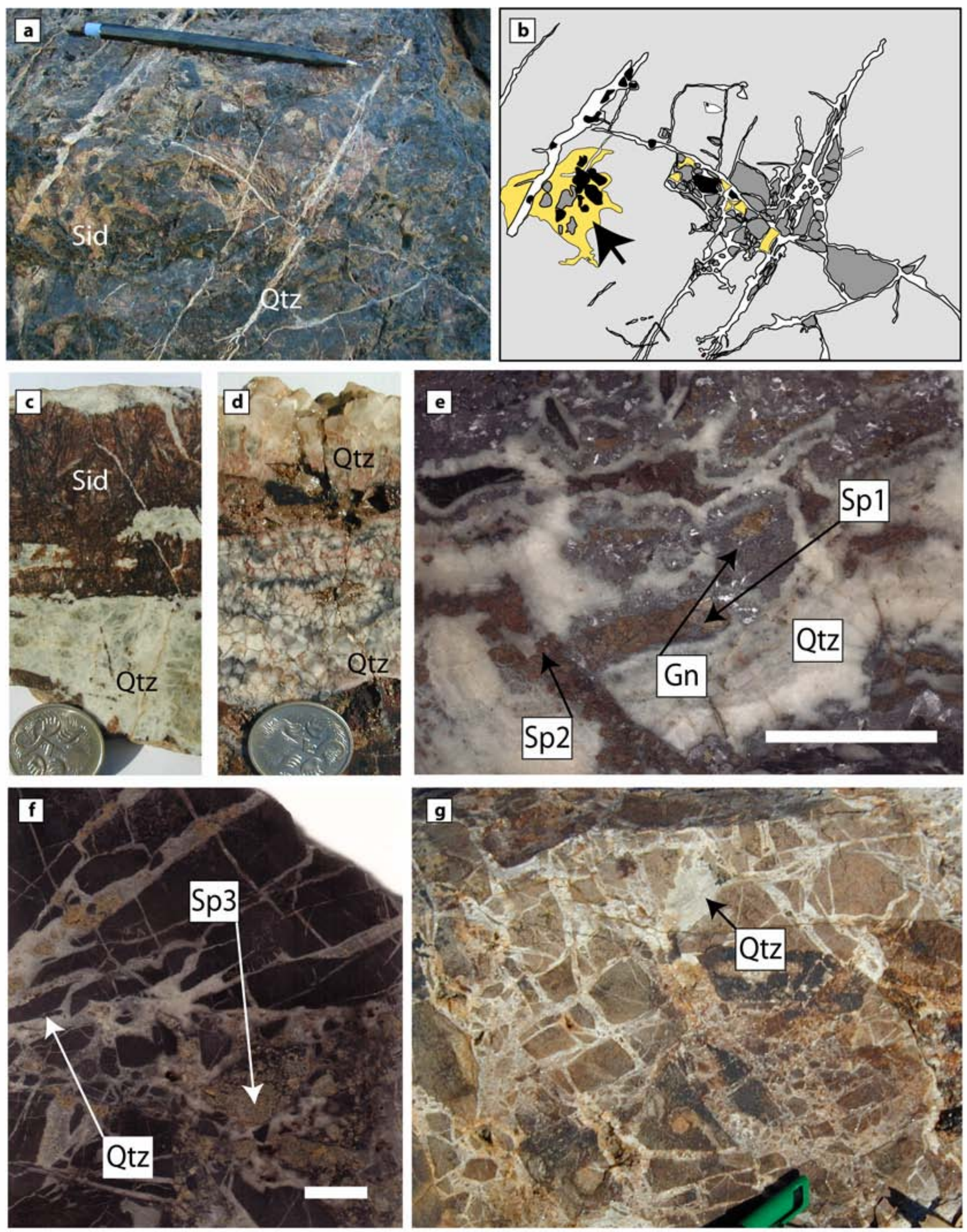

Fig. 3.6 Breccia-style mineralisation and hydrothermal alteration occurring regionally along the Termite Range Fault Zone. (a, b) example of a vein array found at the intersection of NW- and NE-faults and proximal to the Century deposit (star site in Fig. 3.2). Steep dipping quartz veins strikes N140 and are off-set by later parallel bedding shear veins. Vein arrays vary in size from hairline healed fractures to m-scale massive veins. Shear sense indicators suggest apparent sinistral sense of movement. Both quartz-rich vein-sets may be synchronous forming in the same tectonic cycle. However, they postdate an earlier stage of brecciation with more sideritic infill, see arrow in (b). Reddish sideritic cement includes rounded to angular polymictic clasts displaying different degree of REDOX alteration. (c) Paragenetic relationships of quartz

(Qtz) postdating massive crystalline siderite (Sid) at Watson's lode. (d) Comb quartz showing multiple quartz overgrowths, Watson's lode. (e) Colloidal microcrystalline quartz intergrown with sphalerite (Sp) and galena (Gn) (Silver King Mine). Variation in the availability of sulphur may have controlled alternating phases of quartz-carbonates vs. sulphides. Sulphides occur either as vein-infill or angular clasts, suggesting that their emplacement was synchronous with the brecciation. (f) Similar sequence of stages observed in (e) although quartz (Qtz) occurs in veins. (g) and (f), are both examples of hydraulic brecciation (jigsaw breccia in g from moon site, see Fig. 3.2b). This is inferred to have formed during contraction at depth, likely a tectonic component after burial have contributed to elevated pore-pressure values, exceeding the lithostatic stress. Samples (e , f) repolished from Bresser collection (1992) (scale bars in e, f respectively 3.5 and 1 cm).

3.4.1.3. End member relationship between stratiform mineralisation and fault related mineralisation

As seen the two styles of mineralisation recognised have different connotations. Century-style ore occurs predominantly in carbonaceous rocks and its relationship to faulting is somehow ambiguous; whereas, Silver King-style ores are clearly linked to faulting and may occur in a wider range of lithotypes. There is a component of trade-off between these end-members that depends on the genetic overlap existing between the two styles. Deformation and other factors such as diagenesis and metamorphism may cause mixing of the different generations of base metals (e.g. Feltrin and Oliver, 2004). Certain mineralogical textures may reflect a response to the rock's reorganisation due to deformation or other mechanisms involving density variations – remobilisation or mobilisation are then a driven process that follows the entropy laws (e.g. Ortoleva et al., 1993; Park and Ortoleva, 2003). The permeability of a rock mass is an important variable in this context that can be used to asses the degree of self-organisation of a mineral deposit and may help to discriminate its genesis (e.g. a protracted tectonic activity may reorganise mineralisation not previously related to faults).

In this context, the clustering of vein-style deposits observed around Century is considered a plausible indicator of a genetic relationship existing between SEDEX-style mineralisation and inferred later VS deposits. Intuitively, clusters of remobilised sulphide veins are more likely to form where a large reservoir of sulphides is available and proximal, if such a reservoir is accessible to hydrothermal fluids.

3.4.2. Lithological control on mineralisation

The host-rock composition may directly control the chemistry of hydrothermal fluids if the velocity of percolation is sufficiently slow to permit equilibration throughout host rock chemical reactions (Heinrich et al., 1996; Bons, 2001; Oliver, 2001). This section focuses then on the role of lithological variations across the Lawn Hill Region; these have a direct correlation with parameters such as primary and secondary permeability, and also organic, carbonatic (dolomitic) and evaporitic content. These factors influence the solubility of base metals in a solvent (the brine). Therefore, five variables were defined in the KD-probabilistic model to account for the lithological variation: (1) primary permeability, (2) secondary permeability, (3) organic content, (4) presence of maximum flooding surfaces and (5) occurrence of evaporites and dolomites. Model components were combined to generate two different mineral potential models depending upon the style of Pb-Zn mineralisation considered.

Vein style mineralisation (VS) might be interpreted, following Bresser (1992) and Broadbent (1999), as reminiscent of MVT-style mineralisation (Mississippi Valley Type), because most of the veins are inferred to form by hydrothermal solutions that were driven by the orogenic uplift similarly to the groundwater flow model proposed for the

Pine Point deposit in Canada (Garven, 1985). However, the majority of VS ore is not typically MVT-type as it does not occur in carbonates and dolomites within solution collapse breccia (e.g. Anderson, and Macqueen, 1982; Leach and Sangster, 1993). There are only some prospects localised in the Kamarga dome area that do occur in stromatolitic dolomites and might be therefore considered MVT-style or perhaps Irish-style examples (e.g. Kamarga deposits). Available data are however insufficient to confidently classify them. It is therefore used the term VS to avoid misclassification of epigenetic mineralisation. Beside their classification these ores are diverse form classical syngenetic mineralisation. Their strong tectonic imprint is more typical of Irish-style stratabound mineralisation whereas some of the colloform textures observed in fault associated cavities are also typical of MVTs. The five lithological parameters introduced above are briefly discussed emphasising the role they play depending upon the style of mineralisation considered. As discussed below two different KD models are presented and favourability indexes were developed considering also the different role played by the host rock.

3.4.2.1. Primary permeability

Primary permeability (effective porosity) is inferred to be of notable importance for SEDEX-type and early diagenetic mineralisation (e.g. Chen et al., 2003) allowing diffusion of fluids with reasonable transfer velocities, therefore, favouring the development of broad haloes, observed in some of the world class Mount Isa Pb-Zn occurrences (Large and McGoldrick, 1998; Large et al., 2000; Feltrin et al., 2006). Additionally, connected voids associated with primary permeability are the first pathways used during expulsion of fluids due to compaction in a sedimentary basin. Consequently these are frequently filled with cements during diagenesis suggesting that primary permeability is only effective until early stages of burial and compaction. The primary permeability is function of grain size and composition of the host-rock. Grain size controls the initial volume of void space; the rock composition affects the 3D permeability variation and cementation processes. To account for the variation of these parameters the classification of different lithotypes provided by Krassay et al. (2000) and Southgate et al. (2000) was used. A pairwise comparison among the various lithotypes was then adopted to develop a series of expert based scores (see Appendix E) for each lithological unit included in the 100.000 km geological map of the Lawn Hill Region (Fig. 3.1a).

For an early diagenetic, shallow depth system, the primary permeability provides access to extensive volumes of sediments favouring deposition or/and massive replacement of stratal geometries. The discovery of a copper-bearing sulphide replacement horizon of sandy turbidites at approximately 200 m depth in the Juan de Fuca spreading centre (Zierenberg et al., 1998) represent a good example of such early diagenetic replacement. During early stages of sediment deposition aspects such as osmotic pressure may be also particularly important controlling sub-seafloor (re)distribution of mineralisation (see Cheng et al., 2003 for an example of the role of carbonatic layers at the HYC deposit). Primary permeability when connectivity of micro-pores is sufficiently high is then interpreted here as a factor that controls the patterning of sulphides at shallow depths, in conjunction with seafloor deposition of sulphides. In some cases the role of sub-seafloor replacement may be limited in finer sediments leading to patterns exclusively governed by sedimentary deposition of sulphides such as finely laminated bands.

3.4.2.2. Secondary permeability

As soon as the degree of cementation progresses the primary permeability is overcome by secondary permeability enhancement and fluid flow consequently will be focused preferentially along newly formed cavities, stylolites, hydro-fractures, and faults. Secondary permeability can be controlled by dissolution/precipitation processes involving a fluid phase and the host rock. For example, at the Pine Point deposit, Canada, a wide range of open filling, colloform, concretional textures are associated with dissolution cavities developed within a dolomitic host (Anderson and Macqueen, 1982). The worldwide association of Mississippi Valley Type and Irish Type deposits with dolomitic limestone and carbonate-enriched sandstones, in which secondary enhancement of permeability is favoured, was therefore considered one of the major controlling factors for the localisation of VS epigenetic mineralisation in the KD-model.

3.4.2.3. Organic content

There is worldwide evidence of a spatial association of organic matter or hydrocarbons to Pb-Zn mineralisation. For instance, the hydrothermal sites of the Guyamas Basin are present day examples where discharge of metalliferous brines occurs contemporaneously with the formation of petroleum, by cracking of organic matter in the sediments. This occurs in a high-temperature convective regime (Simoneit and Lonsdale, 1982; Rona, 1984). The interaction between sulphides and hydrocarbon occurs either at seafloor or at considerable depth when the maturation of organic compounds is a response to the normal geothermal gradient. A spatial association of sulphides with hydrocarbon is therefore not indicative of formation at certain depths (see also Coveney et al., 2004).

Other more ancient examples of spatial association might be the extensive Viburnum Trend in North America, which is localized at marginal sites within sedimentary basins where organic rich shales and hydrocarbons were abundant (Coveney, 2000). Also within the Northern Australian Craton, evidence of association between organic matter / hydrocarbon and mineralisation has been reported for giant shale-hosted systems such as HYC and Century. Recently, Chen et al. (2003) proposed an interesting analogy between fossil hydrocarbon found in ore and mudstone at HYC (McArthur River), and the previously mentioned oils of the Guyamas Basin, advocating that abundances and distributions of polycyclic aromatic hydrocarbons are linked to hydrothermal gradients formed during ore deposition. At Century, Broadbent et al. (1998) recognised the interaction between small veinlets of hydrocarbon, more likely derived from the organic rich shales (hosting the mineralisation during maturation), and sphalerite. He also proposed a model in which the textural appearance of sphalerite was controlled by the physical state of a hydrocarbon-reservoir (gaseous/liquid phase proportions). In Fig. 3.7a and 3.7b a plot of the stratigraphic variation of metal content across the stratigraphy at Century is presented, which outlines its possible linkage with the organic matter content. A fairly good correlation is apparent, although the multiple possible roles of organic matter and hydrocarbons as reducing agents and as possible sulphur suppliers at different times are arguable. The spatial association observed might be the result of a favourable condition of preservation of both sulphides and oil rich shales. The contemporaneous accumulation of sulphides raining on to the seafloor, in presence of stratified waters with euxinic conditions, does not imply a direct interaction of sulphide bearing brines with organic components (see Goodfellow, 1987; Turner, 1992).

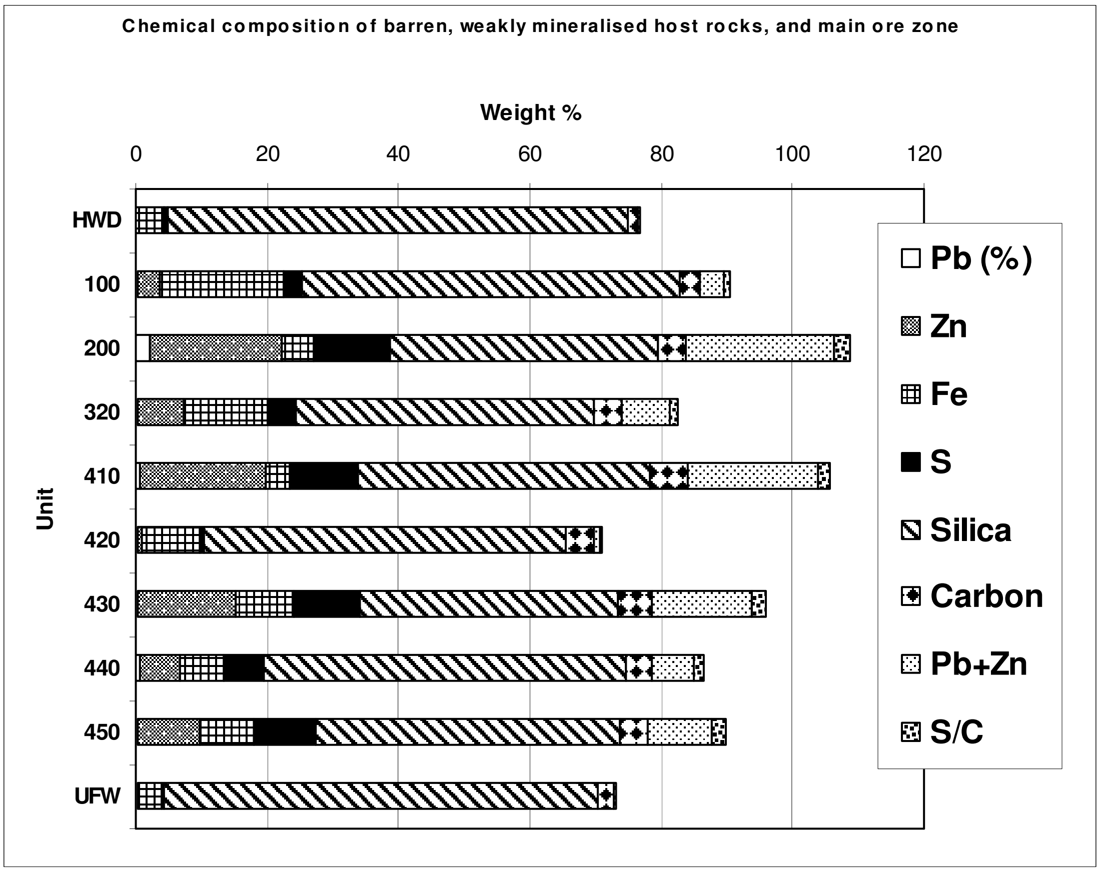

Fig. 3.7a Diagram illustrating the stratigraphic variation of Pb, Zn, Fe, S, Silica, Carbon, Pb + Zn contents, and Sulphur/Carbon ratio (drill core LH412, data from Johnson, 2000). Weight % of base metals (Pb, Zn) and C are covariant. Silica content shows inverse proportional relationship to mineralisation. The sulphur-carbon ratio is indicative either of a hydrothermal supply of exotic sulphur-rich fluids or might be indicative of oscillations from reductive through to oxidative seawater chemical conditions at the seafloor.

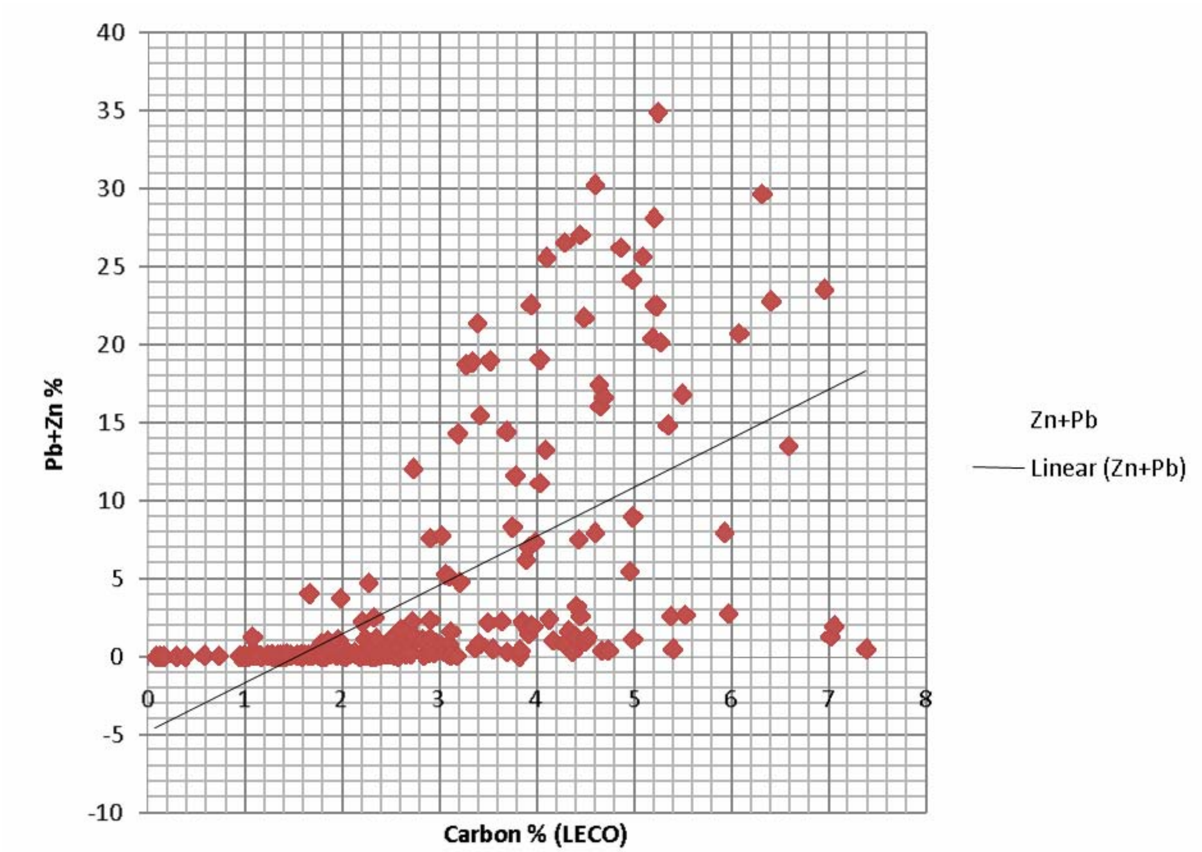

Fig. 3.7b Scatter plot illustrating the correlation between base metals and carbon content (drill-core LH412, data from Johnson, 2000). Despite the scattered distribution the diagram outlines a positive correlation with higher concentrations of Pb+Zn when carbon is above 5%. Low % Pb+Zn are also observed within the same interval; however, they might be interpreted as simple low % zones or outliers. Depletion in some layers may have occurred during diagenesis and local deformation (faults/fractures) lowering the base metal content.

3.4.2.4. Sequence stratigraphic boundaries

The lithostratigraphic formations were reclassified using sequence stratigraphic concepts (Southgate et al., 2000). The use of depositional sequences defines important depositional boundaries such as maximum flooding surfaces, which are sites where syngenetic mineralisation is deposited. Therefore, using the NABRE database composed of an extensive number of drill logs and stratigraphic sections a summary of the number of second and third order maximum flooding surfaces was compiled. Subsequently, increments of expert based scores were applied accordingly to this parameter. Maximum flooding surfaces also represent condensed sections of a sedimentary basin (Fig. 3.8) where orthochemical deposition is favoured as clastic supply is virtually absent. Synsedimentary, metalliferous shales may accumulate in condensed sections, remaining preserved in these intervals (Large, 1988; Ruffell et al., 1998). Within starved basins the slow rates of sedimentation can significantly affect the composition of siliciclastic layers. For example, seasonal oscillations in the pycocline (surface separating oxidised from anoxic seawater) favour the precipitation of Mn-oxides and carbonates as well as controlling the percentage of organic matter preserved during sedimentation (e.g. Algeo and Maynard, 2004).

THIS IMAGE HAS BEEN REMOVED DUE TO COPYRIGHT RESTRICTIONS

Fig. 3.8 Schematic diagram of sequence stratigraphic facies variation in relationship to eustatic oscillations. SEDEX mineralisation is found more likely in condensed section at maximum flooding surfaces. Whereas, MVT-style or Irish-style mineralisation may form proximal to maximum flooding surfaces above and below them. These sites have more permeable carbonatic and sandstone-siltstones dominated packages (redrawn from Ruffell et al., 1998).

3.4.2.5. Presence of carbonates and evaporites

Both the end-members considered (SEDEX, MVT or IRISH) have possible genetic correlation with the occurrence of carbonatic and evaporitic sequences in a sedimentary basin. Carbonates and evaporites form in sabhka lake or epicontinental seas at relatively shallow water depths (e.g. Zechstein Basin of Central Europe). Such restricted conditions increases water salinities (including the concentration of SO_4^{2-}) and also contributes to water stratification that helps the preservation of organic matter at seawater/sediment interface. Within this context, there is a need to differentiate the type of correlation existing between the different styles of mineralisation and this particular association of lithofacies. SEDEX-type deposits are found associated with the organic rich part of these sequences and it has been inferred that some of the sulphur co-precipitated with base metals might be derived directly from the proximal evaporitic sequences. Therefore, the spatial association is indirect, as SEDEX deposits simply share a favourable depositional environment, within which evaporites and dolomitic sequences form. SEDEX-type ore also forms in several other types of settings including deep water siliciclastic environments below wave base, in which dolomitic and evaporitic components are lacking (e.g. Century).

MVT or IRISH mineralisation as pointed out has stronger correlation with carbonatic-evaporitic hosts. Derivation of sulphur from base metal fixation can be inferred similarly to SEDEX although MVT or IRISH mineralisation displays a spatial association with these lithotypes that is of direct type and driven by secondary permeability enhancement. Dolomitic and evaporitic units are easier to dissolve by fluids interacting with them as they are more reactive than siliciclastic rocks.

3.4.3. KD model integration

The knowledge base presented in the previous sections has been utilised to develop numeric scores that helped the standardization of information as constraint for the development of favourability layers. These were subsequently converted to digital form within a 2D-GIS model using the software IDRISI (Clark University, Massachusetts). Two main evidential layers were developed: one based on the structural aspects of the studied region (e.g. scale of half-graben structures) and another based on the parameters discussed for the observed lithotypes. Integration was achieved using an Ordered Weights Average (OWA) approach that ranks the factors utilised to establish mineral potential plausibility. This method allows more control on risk analysis and trade-off between the different lines of evidence considered within the model (Eastman, 1999; Yager, 1988).

Most problems approached with a GIS are multi-criteria in nature. Our concern lies with how to combine these criteria to arrive at a composite decision. As a consequence, the first major area of concern in GIS with regard to Decision Theory is Multi-Criteria Evaluation. In the case of Boolean criteria (constraints), the solution usually lies in the union (logical OR) or intersection (logical AND) of conditions. However, for continuous factors, a weighted linear combination (Voogd, 1983) is most commonly used. With a weighted linear combination, factors are combined by applying a weight to each followed by a summation of the results to yield a suitability map, i.e., $S = \sum w_i x_i$, where S = suitability, w_i = weight of factor i, x_i = criterion score of factor i. Because of the different scales upon which criteria are measured, it is necessary that factors be standardized before combination using the formula above, and that they be transformed, if necessary, such that all factors maps are positively correlated with suitability. Voogd (1983) reviews a variety of procedures for standardization, typically using the minimum and maximum values as scaling points. The simplest is a linear scaling such as: xi = (Ri-Rmin) / (Rmax-Rmin) * standardized range, where R = raw score. However, if we recognize that continuous factors are really fuzzy sets, we easily recognize this as just one of many possible set membership functions. In IDRISI, the module named FUZZY was used for the standardization of factors using a whole range of fuzzy set membership functions. The module provides the option of standardizing factors to either a 0-1 real number scale or a 0-255 byte scale. Once the standardisation is completed a wide variety of techniques exist for the development of weights that need to be assigned to the relative factors (favourability layers). In very simple cases, assigning criteria weights may be accomplished by dividing 1.0 among the criteria. However, when the number of criteria is more than a few, and the considerations are many it becomes quite difficult to make weight evaluations on the set as a whole. Breaking the information down into simple pairwise comparisons in which only two criteria need to be considered at a time can greatly facilitate the weighting process, and will likely produce a more robust set of criteria weights. A pairwise comparison method has the added advantages of providing an organised structure.

Once the criteria maps have been developed, an evaluation (or aggregation) stage is undertaken to combine the information from the various factors and constraints. Three logics for the evaluation/ aggregation of multiple criteria are commonly applied: Boolean intersection, weighted linear combination (WLC – firstly developed by Saaty, 1977), and the ordered weighted average (OWA).

- The most simplistic type of aggregation is the Boolean intersection or logical AND. This method is used only when factor maps have been strictly classified into Boolean suitable/unsuitable images with values 1 and 0. The evaluation is simply the multiplication of all the images. The derivation of criterion (or factor) weights is described above.
- The weighted linear combination (WLC) aggregation method multiplies each standardized factor map (i.e., each raster cell within each map) by its factor weight and then sums the results. Since the set of factor weights for an evaluation must sum to one, the resulting suitability map will have the same range of values as the standardized factor maps that were used.

- In its use and implementation, the ordered weighted average approach is not unlike WLC. The OWA method is almost identical to that of WLC, with the exception that a second set of weights appears. This second set of weights, the *order weights*, controls the manner in which the weighted factors are aggregated (Eastman and Jiang, 1996; Yager, 1988). Indeed, WLC turns out to be just one variant of the OWA technique.

To better explain the OWA technique, it is instructive to firstly review WLC in terms of two new concepts: tradeoff and risk.

- **Tradeoff:** factor weights are weights that apply to specific factors, i.e., all the pixels of a particular factor image receive the same factor weight. They indicate the relative degree of importance each factor plays in determining the suitability for an objective. In the case of WLC the weight given to each factor also determines how it will tradeoff relative to other factors. For example, a factor with a high factor weight can tradeoff or compensate for poor scores on other factors, even if the unweighted suitability score for that highly-weighted factor is not particularly good. In contrast, a factor with a high suitability score but a small factor weight can only weakly compensate for poor scores on other factors. The factor weights determine how factors tradeoff but, as described below, order weights determine the *overall* level of tradeoff allowed.

- **Risk:** Boolean approaches are extreme functions that result either in very risk-averse solutions when the AND (multiplication of layers) operator is used or in risk-taking solutions when the OR (addition) operator is used. In the former, a high aggregate suitability score for a given location (pixel) is only possible if *all* factors have high scores. In the latter, a high score in any factor will yield a high aggregate score, even if all the other factors have very low scores. The AND operation may be usefully described as the *minimum*, since the minimum score for any pixel determines the final aggregate score. Similarly, the OR operation may be called the *maximum*, since the maximum score for any pixel determines the final aggregate score. The AND solution is *risk-averse* because we can be sure that the score for every factor is at least as good as the final aggregate score. The OR solution is *risk-taking* because the final aggregate score only tells us about the suitability score for the single most suitable factor. The WLC approach is an averaging technique that softens the hard decisions of the Boolean approach and avoids the extremes. In fact, given a continuum of risk from minimum to maximum, WLC falls exactly in the middle; it is neither risk-averse nor risk-taking.

- **Order Weights, Tradeoff and Risk:** the use of order weights allows for aggregation solutions that fall anywhere along the risk continuum between AND and OR. Order weights are quite different from factor weights. They do not apply to any specific factor. Rather, they are applied on a pixel-by-pixel basis to factor scores as determined by their rank ordering across factors at each location (pixel). Thus, it is possible that a single order weight could be applied to pixels from any of the various factors depending upon their relative rank order. To examine how order weights control levels of tradeoff and risk, let us consider the case where factor weights are equal for two factors A and B. For instance A = B = 10 gives a vector x = [10, 10]. If it is adopted the following set of order weights y = [1, 0] the final outcome of a combination would give a result in the final aggregation z = 10. If we consider another example in which y = [0.5, 0.5] we would obtain the same result. However, in this case this is due to the initial assumption of having equal factor weights. The main difference between these simple examples is that order weights in the first case are forcing the final result of a layers combination to be conditioned heavily by the first factor. In the second example order weights are essentially in full tradeoff. In other words, the degree of tradeoff is governed by the relative distribution of order weights between the ranked factors. Thus, if the sum of the order weights is evenly spread between the factors, there is strong tradeoff, whereas if all the weight is assigned to a single factor rank, there is no tradeoff. In addition to the tradeoff concept, favourability layers are combined using a compromise between Boolean OR/AND operations. Using OWA makes these rules less restrictive because the use of order weights allows to control the risk condition. For example, in case of full tradeoff (which means spread order weights across the different factors) the model is forced in the middle of the risk continuum, resembling a softer solution equivalent to a WLC approach.

Two probabilistic models are presented, one for SEDEX and one for VS deposits. The outcome is represented by plots of stratigraphic potential and maps of predictability for SEDEX type ore, and VS ore. There is an implicit overlap between these end-members, although the end-member subdivision was valuable for exploring the relationship between geological complexity and spatial distribution of known mineral occurrences.

By analogy with the data-driven model (DD), an expert-driven model is a two-fold process that involves a preliminary phase of data standardization and subsequent phase of data assembly. Usually the criteria considered (evidential layers) are distinguished as constraints or factors. These are respectively considered hard and soft components of a KD-model. Structure and lithology were represented in a binary format (Boolean constraints), whereas continuous variation of favourability was approximated utilising fuzzy membership functions (see Bonham-Carter, 1994). These latter constitute a softer approach that allows a certain degree of trade-off depending on the function adopted and the type of aggregation method (see below).

Different assumptions were utilised for the SEDEX and VS models. The SEDEX model considered a fault database composed of three main groups (NE, NW, E-W). These were used to create independent evidential layers that were combined using an OWA (Ordered Weighted Average) with ranking coefficients of (0.4, 0.3 and 0.3) respectively for NE, NW, E-W faults. This assumption gives more weight to NE structures as they were considered normal dip-slip faults that are interpreted as older growth faults (Broadbent et al., 1998; Betts and Lister, 2002). Within a SEDEX context these structures may have contributed as sources for mineralising fluids during synsedimentary tectonic activation. However, the chosen weights are a full trade-off that reflects the level of uncertainty of this assumption. NW and E-W faults may have been important as well and other variables may have been conditioning the relationship between structure and mineralisation (e.g., fault intersections in case of fluid mixing). SEDEX deposits do not necessarily form proximal to faults (e.g. Rona, 1984), e.g. brine pools may migrate towards deeper parts of starved basins away from faults although the range of mobility is restricted by the scale of half-graben developed during syn-rift activity or sagging. A buffer of 5km was used as the maximum distance from the faults to take into account these considerations. This assumption could be important, as identification of resources away from major faults may be a discriminator between SEDEX and VS ore. A different set of assumptions was considered valid for VS deposits: equal order weights were adopted for all the sub-groups of faults reducing the OWA to its full trade-off end-member, which is the equivalent of a weighted linear combination (WLC) model in which ranking coefficients are equal. A Boolean buffer of 1km, a risk-averse choice compared to the wider buffer previously adopted, was chosen because proximity to faults is more important for this style of mineralisation, as secondary permeability enhancement is the main spatial constraint.

3.4.3.1. Assumption for lithotype-based evidential layers

A similar procedure to the previous standardization of structural layers was utilised to develop the lithotypes based evidential layers. Two layers (SEDEX, VS) were developed. The number of variables considered was higher than in the previous model. To help the development of weighting coefficients, five independent criteria were defined: primary and secondary permeability, organic content, carbonate/evaporite content and number of maximum flooding surfaces. Initial pairwise comparison of lithotypes led to the definition of primary permeability scores; a subsequent phase involved the update of these initial values. Fig. 3.9 summarises the assumptions made and presents the workflow utilised (see also Appendix E - CD folder).

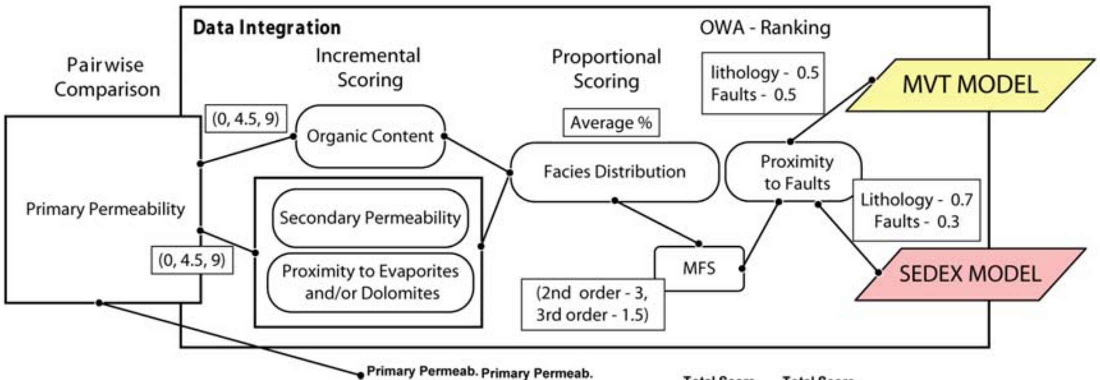

	Primary Permeab. Score (SEDEX)	Primary Permeab. Score (MVT)	Total Score (SEDEX)	Total Score (MVT)
Bre	0.5	17.5	5	26.5
C-Sh	15	3	24	7.5
Che	17.5	0.5	22	18.5
Cg	0.5	17.5	0.5	22
Cr-dol	17	1	21.5	14.5
D-mud-sts	11.5	6.5	16	20
D-mud-gra-str	9	9	13.5	27
San-Sts_str	5.5	12.5	10	30.5
Dololut	10.5	7.5	15	12
L-San	2.5	15.5	7	15.5
Carb-Qtz-San	8	10	12.5	28
Qtz-San	2.5	15.5	2.5	15.5
Qtz-San-Dolst	5	13	9.5	26.5
Dolosts-sh	12	6	21	15
Sh	15	3	24	7.5
Sts	7	11	11.5	11
Sts-San	5	13	9.5	13
Sts-Sh	12	6	21	6
T	14.5	3.5	14.5	3.5

Fig. 3.9 Schematic diagram portraying different phases of expert-driven weighting. Initial phases involved development of numerical scores based on pairwise comparison of primary permeability of different lithotypes. Incremental scoring is used in a second phase to account for the organic content, secondary permeability variation and relative content of evaporites and dolomites. Proportional scoring uses a qualitative estimate (average %) of the spatial distribution of lithofacies within each considered stratigraphic interval. The final models (SEDEX, VS) considers also additional scores for occurrence of maximum flooding surfaces and proximity to faults (see text).

Assumptions regarding the primary permeabilities considered impermeable rock types more favourable to SEDEX-style ore, whereas permeable units were assumed to be advantageous for VS ore. For the VS model, the role of secondary permeability enhancement increased the scores as a consequence of the solubility of the carbonate/evaporite content. The importance of organic content and the number of maximum flooding surfaces were used to increment the weights in the SEDEX model, because of the well-known spatial association between base metals and organic rich intervals as previously discussed. The outcome was a classification of all the lithotypes in term of mineral potential for SEDEX and VS deposits (Fig. 3.10). The lithostratigraphic classification of the Lawn Hill area was utilised as a reference for the spatial distribution of outcropping lithologies. Mapped geological intervals are composed of different predominant lithotypes; therefore, using available data (more than 80 sites among regional drill-holes and stratigraphic sections from Southgate et al. 2000 and Krassay et al. 2000) an averaged weight of mineral potential per unit was estimated, considering the relative abundance of each lithotype.

3.4.3.2. Aggregation of evidence

Standardized information relative to structure (spatial distribution of faults) and lithology was assembled performing pixel based algebra in GIS, firstly multiplying the raw-evidence layers by the developed weights and subsequently summing up the values of partial probabilities. An ordered weights average (OWA) was favoured as it allows ranking of criteria (evidence themes). Additional ranking based weights were developed during aggregation of the SEDEX lithostratigraphic model with the fault-layers. Lithological control was favoured rather than the spatial association to faults, assigning respectively ranking coefficients of 0.7 and 0.3 (Fig. 3.9), emphasising the role of lithological variations as SEDEX can be formed away from the faults. No ranking was utilised for the VS model as structure and lithology were considered equally important. The resulting models and enlargements of four subsets are shown in Fig. 3.11a, b, c, d and e.

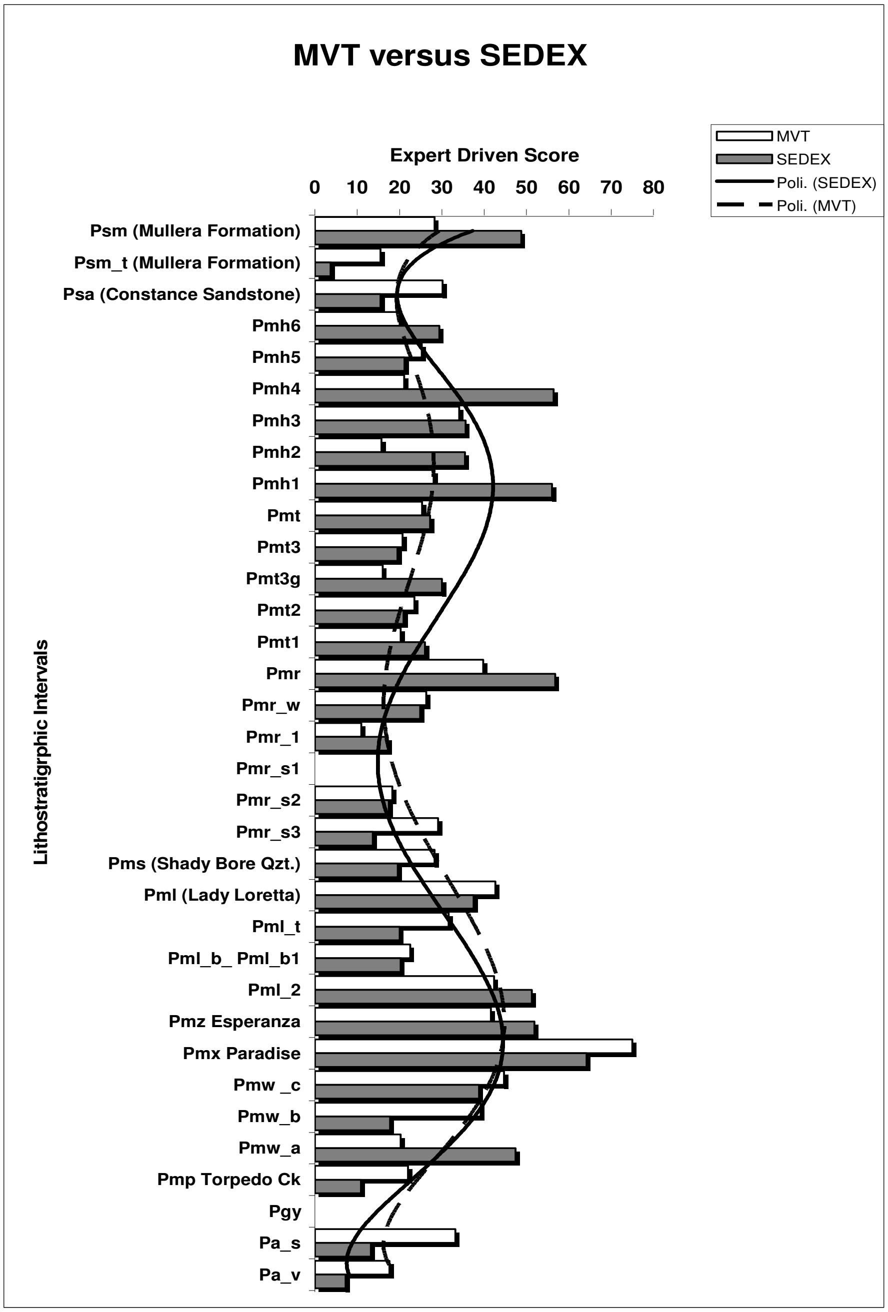

Fig. 3.10 Summary of lithostratigraphic mineral potential for the Lawn Hill Region. Comparing SEDEX potential with VS potential it is noted that the upper part of the sequence (Lawn Hill Fm – Riversleigh Fm.) is more favourable to SEDEX-style mineralisation. In the lower part of the sequence (in particular Lady Loretta, Esperanza and Paradise Creek Fm.) the comparison suggests that mineral potential is high for both styles of mineralisation.

3.4.3.3. Interpretation

The KD-model results can be used as multi-objective tools. The purpose was to evaluate the spatial distribution of the variables considered within the model against known distribution of deposits and prospects in the region to their relationships to prospects/deposits. The following interpretation is proposed based on the KD model.

SEDEX potential is widespread (see Fig. 3.11a) suggesting that suitable conditions for the formation and preservation of exhalative to early diagenetic deposits may occur in different depositional settings. More prospective units (favourability score above 35) were: Psm, Pmh4, Pmh3, Pmh2, Pmh1, Pmr, Pml, Pml_2, Pmz, Pmx, Pmw_c, Pmw_a (see Fig. 3.1a for location).

Comparing the SEDEX prospectivity map of Fig. 3.11a (notice that favourability scores have been rescaled within an interval [0, 256] in all maps) against known mineral deposits/prospects, there was evidence of good agreement of mineralised sites and highest score of favourability in the KD-model although in some cases occurrences intersecting low-favourability fields are recorded. Note that known mineral occurrences include only a single, discovered, shale-hosted giant system (Century deposit – arrow in Fig. 3.1a, b); therefore, most of the prospects and small mines are structurally controlled veins and lodes that however might be proximal to major stratiform deposits. For instance, Century is occurring within a cluster of vein style occurrences. This might indicate that correlation of clusters of VS systems within prospective units is a discriminating factor for SEDEX-type ore; therefore, prospective areas were restricted based on this criterion in two targets, the Century subset and the Kamarga subset (Fig. 3.11a and 3.11b).

The VS-KD model (Fig. 3.11b) indicates that VS occurrences should be preferentially hosted in stratigraphic units outcropping in the southeastern part of the Lawn Hill map. This is also evident on the histogram that outlines mineral potential (Fig. 3.10). Particularly prospective are the Lady Loretta, Esperanza, Paradise Creek Formations and part of the Gunpowder Creek Formation. There is a major peak occurring within the Paradise Creek Formation although this may be the result of a bias related to input data (see below). Localised peaks in mineral potential occur also within the Pmh3 and Pmr intervals, but overall the background appears to be lower compared to SEDEX prospectivity. Comparing the VS-KD model with known mineral occurrences it is noted that only 20 occurrences are localised within or proximal to units with a favourability higher than 0.75. This suggests that the likelihood of finding a VS deposit is higher in the Kamarga Dome area, and south of it. Most of the known deposits/prospects occur within the 1km fault buffer, confirming their structural control.

- Although both KD-models allow definition of favourability maps for distinct styles of mineralisation, there is a clear overlap existing between them. Therefore, with this approach it is possible to delineate the areas with high favourability for SEDEX-style mineralisation, but the result is only a likelihood estimate. Various limitations apply, for instance, the approximation relative to the classification of lithotypes- often too simplistic. A more detailed classification would be a requirement to increase the power of prediction. The analysis is also limited spatially to outcropping lithologies. Favourability scores are derived from assumptions made upon measured stratigraphic sections and available drill-holes. Therefore, the component of uncertainty involved is often difficult to quantify.

These issues can be partly overcome developing a Data-Driven model that uses additional information and permits quantification of the uncertainty related to the missing information. It should also be realised that in KD modelling, operator-bias in assignment of scores is subjective (i.e. no two experts will give the same scores to the same evidence), and uncertainty due to operator bias is also difficult to quantify (Carranza, pers. comm.).

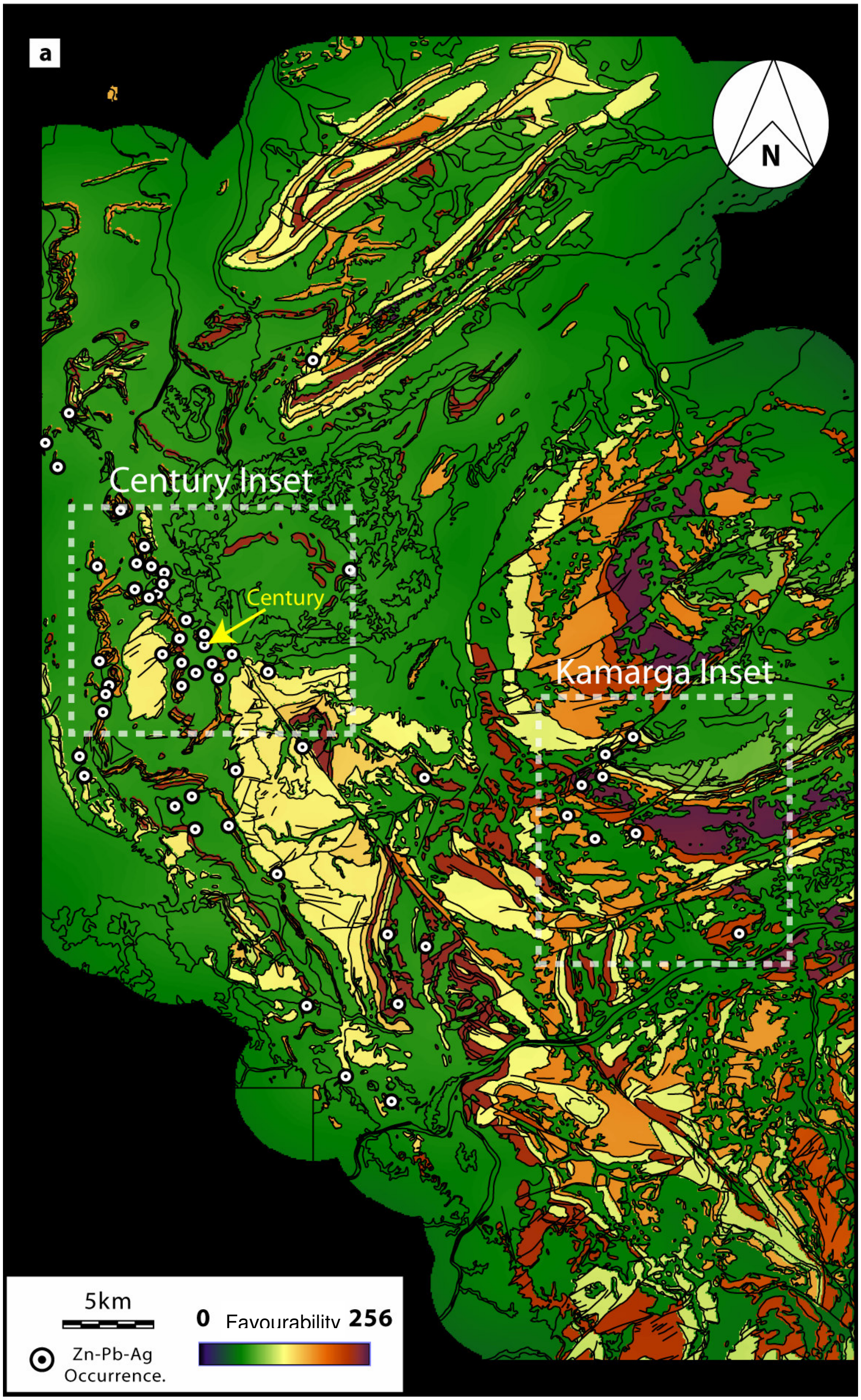
a
N
Century Inset
Century
Kamarga Inset
5km
Zn-Pb-Ag
Occurrence.
0 Favourability 256

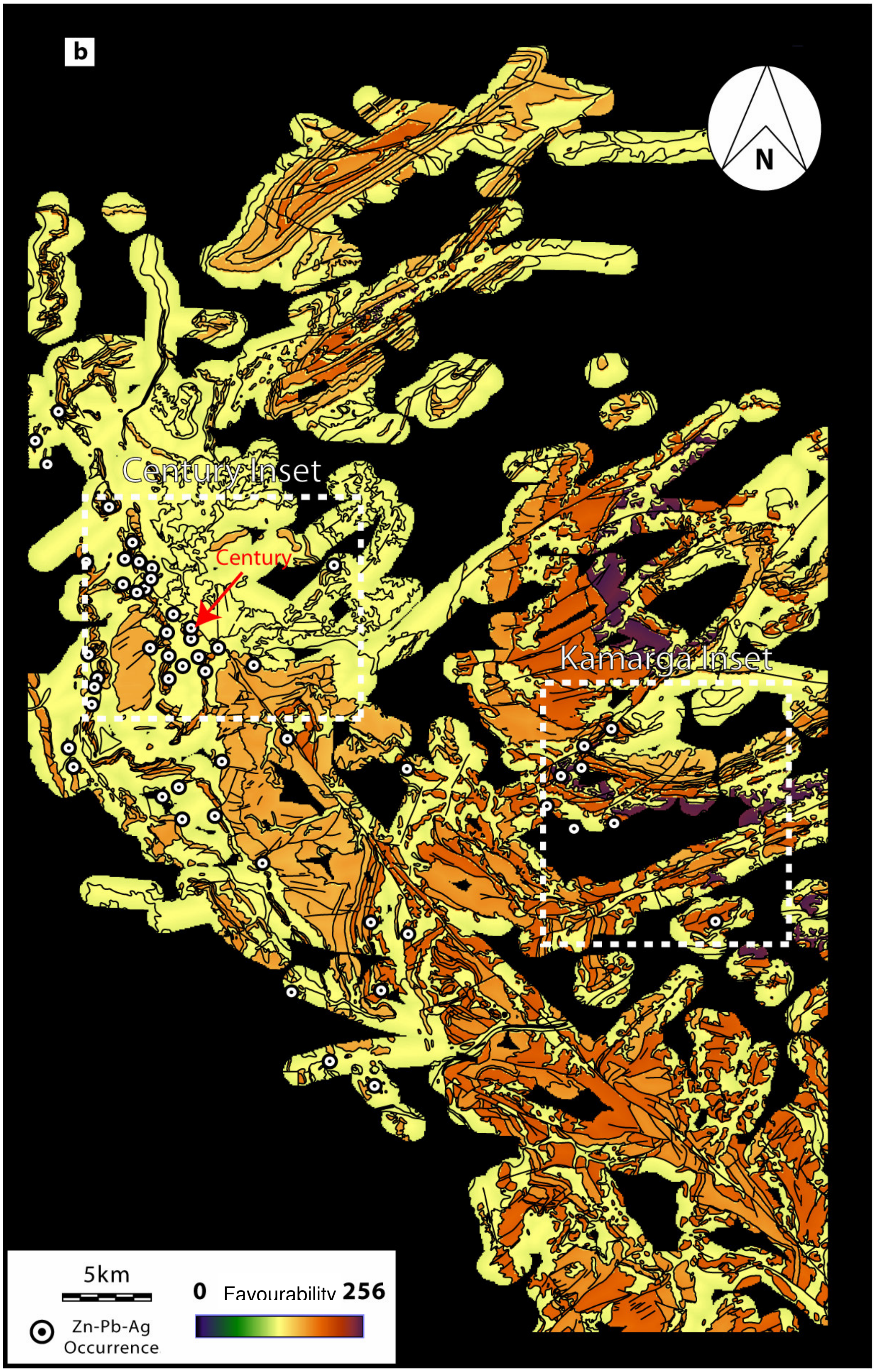
b
N
Century Inset
Century
Kamarga Inset
5km
0 Favourability 256
Zn-Pb-Ag
Occurrence

(c)

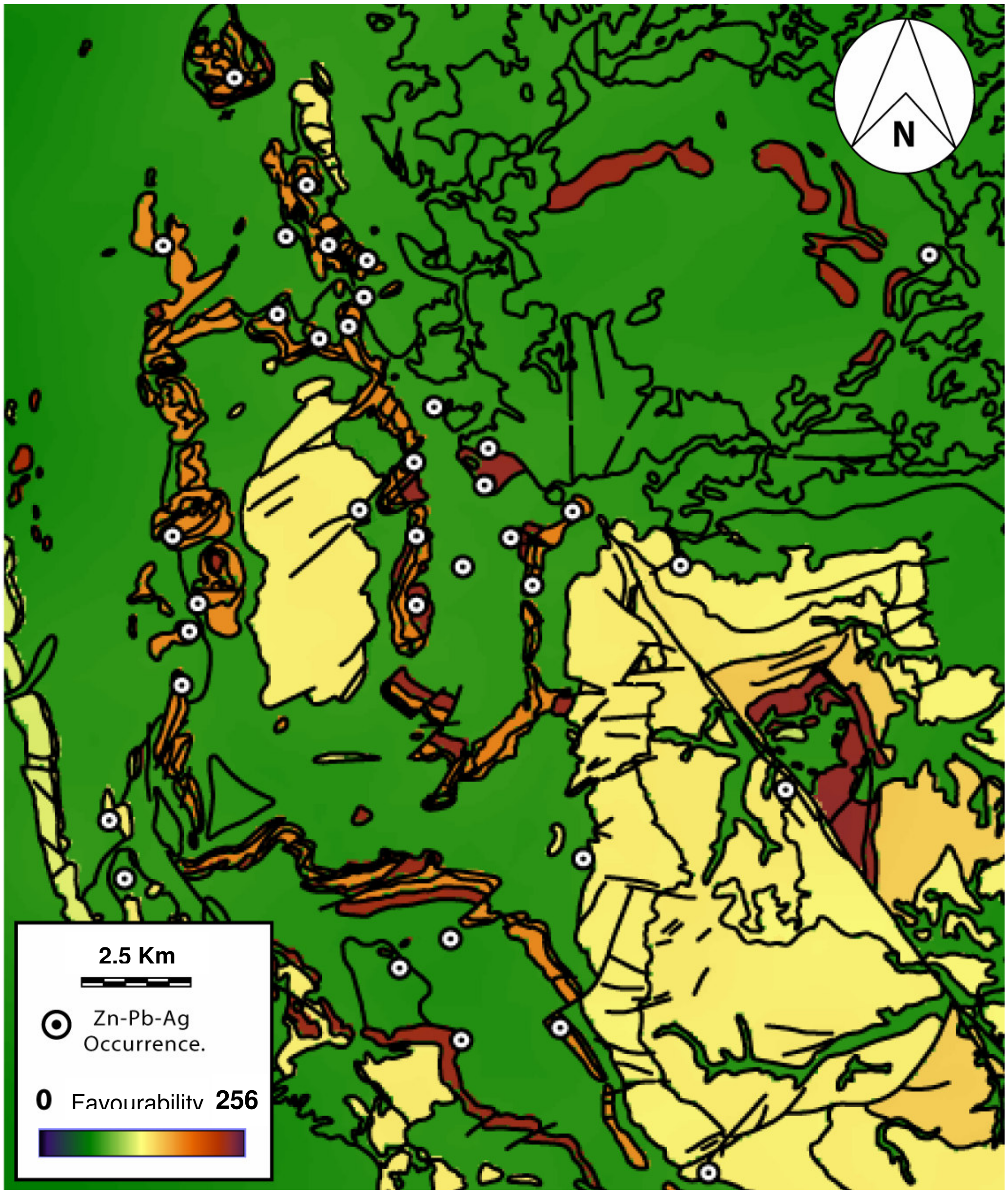

(d)

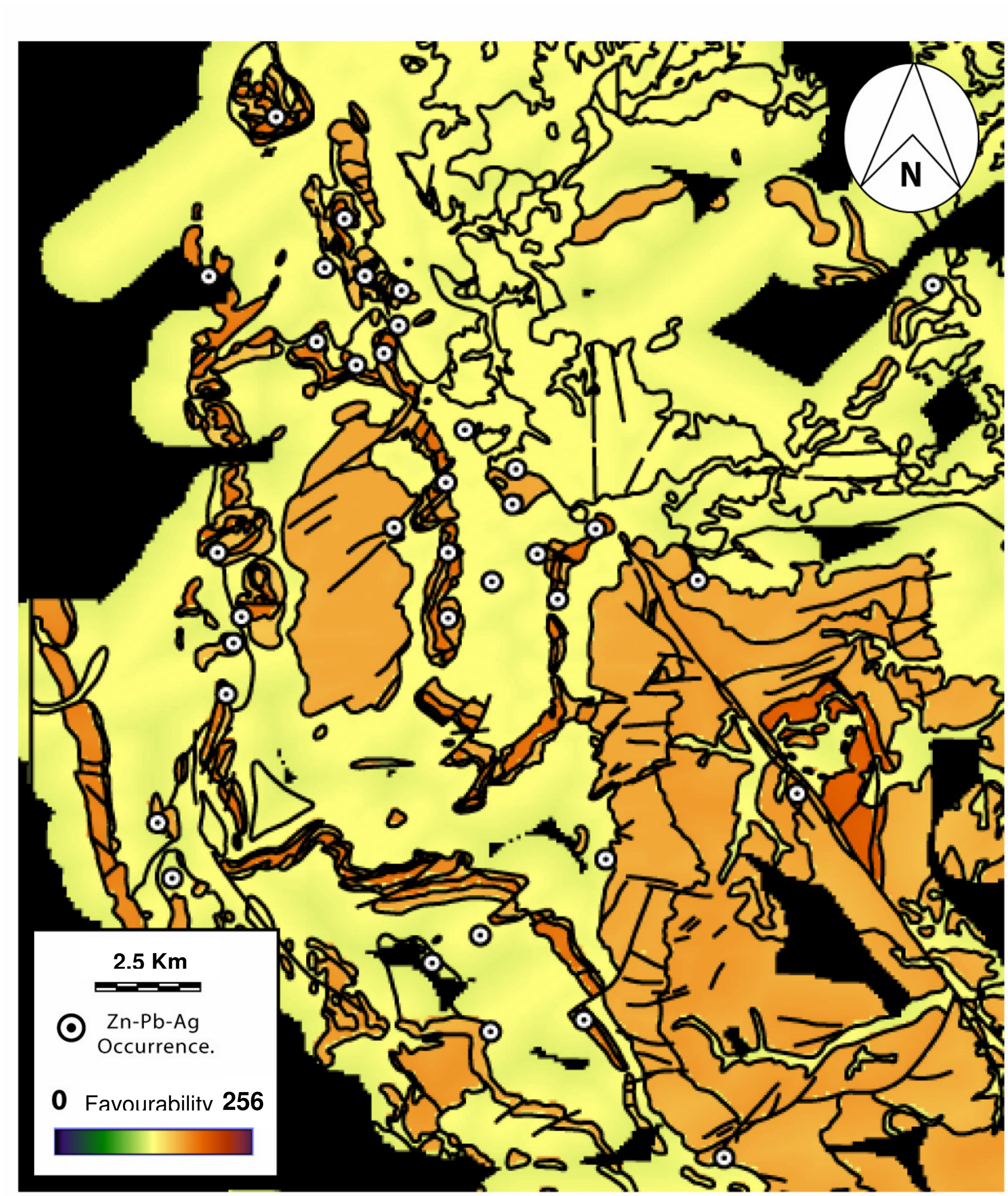

(e)

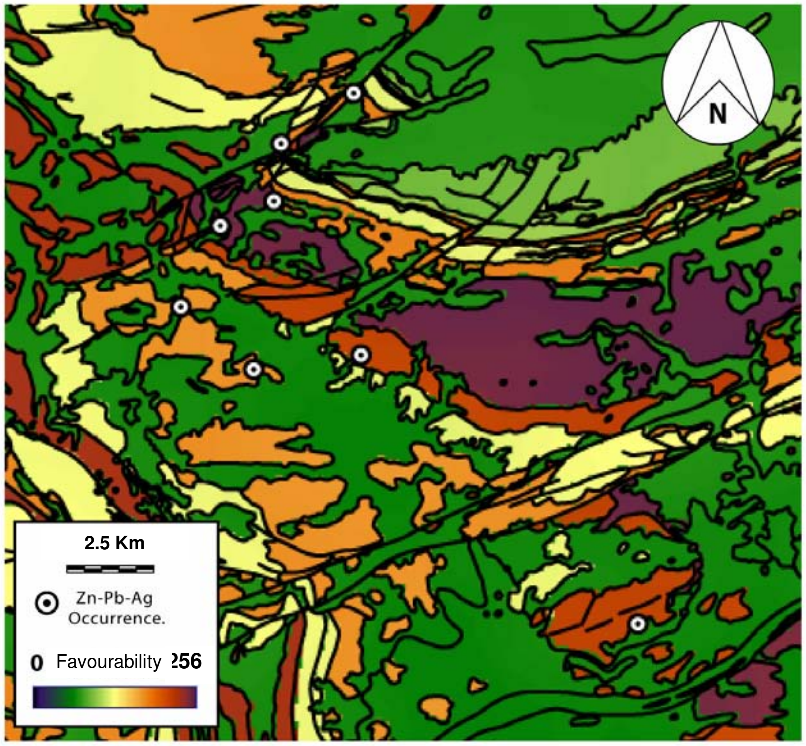
N
2.5 Km
Zn-Pb-Ag
Occurrence.
0 Favourability 256

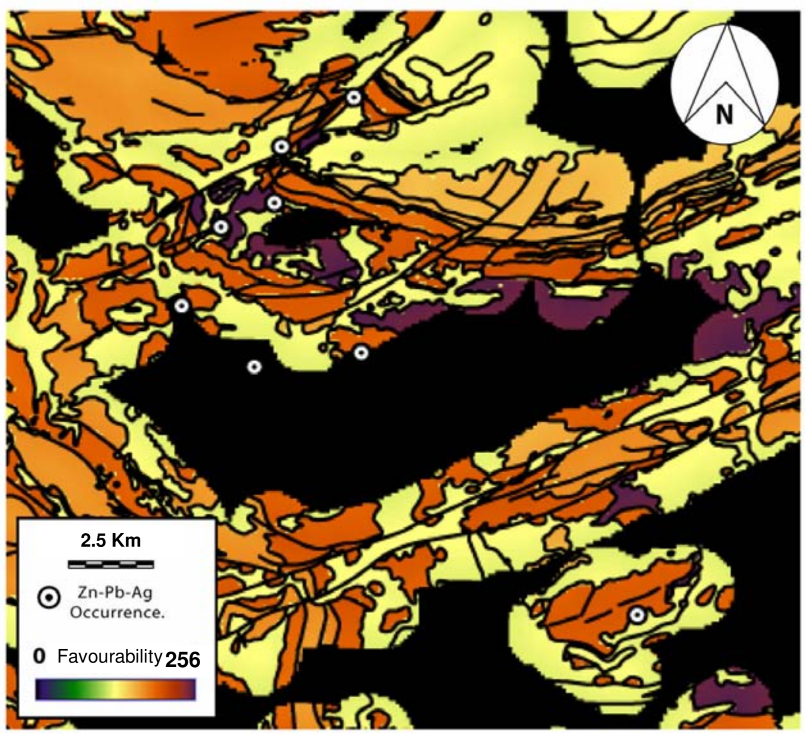
N
2.5 Km
Zn-Pb-Ag
Occurrence.
0 Favourability 256

Fig. 3.11 Maps of mineral potential derived from KD-modelling compared against known distribution of mineral occurrences. (a) SEDEX model shows that known deposits are localised within areas where less-permeable units are present. Favourability is dominated by lithological variation rather than fault control (note large 5km fault buffering). The model is not restrictive therefore wide areas may have potential for SEDEX-type mineralisation in the region. However, if we consider the relationship to clusters of small tonnage deposits and Century, the prospectivity may be constrained to areas where a similar spatial association occurs (e.g. the Kamarga Dome Area). This area records also elevated lithostratigraphic potential. (b) VS model with equal weighting for faults and lithological control (1km buffer chosen for faults). Most of the prospect/deposits occur in the northwestern part of the Lawn Hill Region. In contrast, the KD-model output for VS ore predicts the occurrence of mineralisation in the southeastern part of the Lawn Hill Region. This may be explained either as due to relative undiscovered sites in the favourable intervals or to local redistribution of syngenetic mineralisation that would justify the linkage of VS deposits to Century-style mineralisation in less favourable areas. (c, d, e) Enlargements showing chosen subsets with relative clusters of deposits/prospects.

3.5. Data driven modelling

The Weights of Evidence approach (WofE) (reviewed in Spiegelhalter, 1986; Bonham-Carter, 1994) was utilised to develop a Data-Driven model for the Lawn Hill Region. An advantage derived from the objectivity of this method is its exploratory nature. As it will be demonstrated in the following sections, the spatial association between known deposits and other geological patterns can be explored in detail using the WofE approach. This method, rather than relying on expert knowledge, defines the probability distribution of each evidential layer by estimating a positive and a negative weight for the degree of spatial association existing between the area distribution of deposits/prospects, and the pattern considered.